COMPARISON OF GENE EXPRESSION IN ABDOMINAL AND CARDIAC ADIPOSE TISSUE OF THE MODERN BROILER CHICKEN

By

Blair K. Schneider

A thesis submitted to the Faculty of the University of Delaware in partial fulfillment of the requirements for the degree of Honors Bachelor of Science in Biological Sciences with a Concentration in Cell and Molecular Biology and Genetics with Distinction

Spring 2017

COMPARISON OF GENE EXPRESSION

IN ABDOMINAL AND CARDIAC

ADIPOSE TISSUE

OF THE MODERN BROILER CHICKEN

By

Blair K. Schneider

Approved: _____

Carl J. Schmidt, PhD
Professor in charge of thesis on behalf of the Advisory Committee

Approved: _____

Behnam Abasht, PhD
Committee member from the Department of Animal and Food Sciences

Approved: _____

Robert Dyer, PhD
Committee member from the Board of Senior Thesis Readers

Approved: _____

Michael Arnold, Ph.D.
Directory, University Honors Program

ACKNOWLEDGMENTS

This material is based upon work supported by the National Science Foundation under Grant No. 1147029 and by the Agriculture and Food Research Initiative Competitive by NIFA 2010-04233 from the USDA National Institute of Food and Agriculture. This project was done in collaboration with Dr. Susan Lamont at Iowa State University. A special thanks to Max Manse for performing the RNA extractions. Thank you to everyone in the Schmidt lab for training and aiding me in conducting this experiment. Finally, thank you to Dr. Carl Schmidt, the principle investigator, for overseeing this entire project and bringing it to its full potential along with helping me grow as a scientist. I would not be where I am today without you.

TABLE OF CONTENTS

LIST OF TABLES

LIST OF FIGURES

ABSTRACT

Adipose tissue is a major storage depot for lipids. The chicken has two main fat pads, the cardiac and abdominal fat pads. It is hypothesized that there is a difference in gene expression between the two types of adipose tissue, particularly in genes involved in lipid regulation, reflecting a difference in function. Illumina transcriptome libraries were prepared from Ross 708 market age modern broiler chicken abdominal and cardiac adipose samples. Bioinformatic analysis identified pathways common to both types adipose, unique to abdominal fat, and unique to cardiac fat. Energy homeostasis and lipid regulation appears to be the same in the abdominal and cardiac adipose. The maintenance of the extracellular matrix (ECM) and the microenvironment is also similar between both types of adipose with the cardiac adipose ECM appearing slightly more static. This could be because the cardiac adipose is not the primary lipid storage depot and thus less transport needs to take place within the tissue. The immune responses appear to be different between abdominal and cardiac adipose. The abdominal adipose appears to be slightly more pro-inflammatory while the cardiac adipose appears to be dampening inflammation. Both types of adipose regulate inflammation in unique ways. The abdominal adipose also appears to be upregulating endocytosis, supporting its role as the primary lipid storage depot of the body.

Chapter 1

INTRODUCTION

Adipose tissue is the major storage depot for lipids, where they remain until required as a source of energy for the body (1). Some organs, such as the heart, utilize lipids as their primary energy source (2). Lipids and fatty acids, including those stored in adipose, are also utilized as the primary energy source for the body when glucose supplies are inadequate (1). There are two main fat pads in the chicken: the abdominal fat pad, which is above the GI tract, and the cardiac fat pad, that rest on top of the heart's atria and surrounds the aorta (Figure 1). There is a distinct color difference in the two fat pads, with the abdominal appearing to have a more whitish color and the cardiac appearing to have a more yellow color. This difference led to the question: Are the two types of fat functioning differently? It is hypothesized that there is a biologic difference between the abdominal and cardiac adipose in the modern broiler chicken and clues to this difference can be obtained by describing the gene expression patterns in the two types of fat.

While the cardiac fat is known to act as an energy source for the heart, it is also thought that this fat pad may also function as a cushion to absorb excess free fatty acids (FFAs) preventing lipid overload in the organ (3–5). The function of the abdominal fat pad is serving as the primary storage depot for lipids within the body and regulating their transport (6). Thus, the goal of this study is to determine if predicted differences in abdominal and cardiac fat pads are discernable through analyzing the gene expression pattern of these two types of adipose tissue.

Adipose tissue also is a functioning member of the immune system. A variety of immune cells including: macrophages, neutrophils, eosinophils, mast cells, T cells, B cells, and natural killer (NK) cells, that function in adaptive and innate immunity, can be found in adipose tissue (7). Apparently, ten percent of the total macrophages in both humans and mice can be found within the adipose tissue and their level can increase with obesity (8). The main function of the immune cells within adipose tissue is the regulation of inflammatory responses (7). There are immune cell types that function in pro-inflammatory responses including, mast cells, CD8 T cells, and type 1 helper cells (Th1), and anti-inflammatory responses, (M2) macrophages, regulatory T cells (Treg), and eosinophils (7). Many of the pro-inflammatory responses increase with an increase in fat deposition (7). Consequently, a second goal of this study is to explore the differences in immune gene expression patterns between the two types of adipose tissue.

An RNA- sequencing (RNA-seq) analysis of both abdominal and cardiac adipose tissue in the broiler chicken was performed to test this hypothesis. Genes unique to each type of adipose tissue were identified through a relative tissue expression (RTE) analysis, comparing the expression levels of each gene in each type of adipose to expression levels in the rest of the body. Analysis of these unique genes was performed to correlate gene expression differences to biologically and metabolically significant pathways, with a focus on and genes involved in adipose regulation and immune functioning.

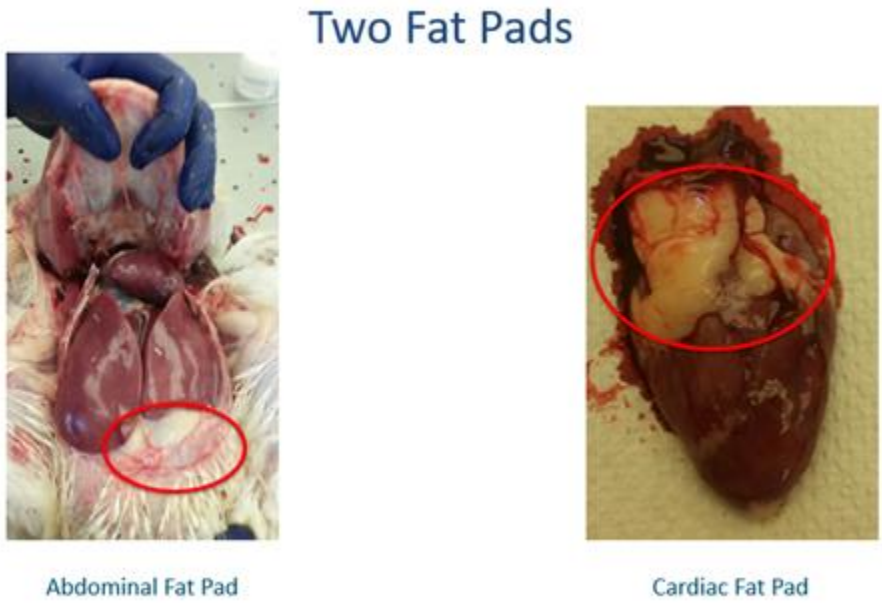

Figure 1: Two main adipose depots (i.e. fat pads) present in broiler chickens. The abdominal fat pad is shown on the left, beneath the liver, and the cardiac fat pad is shown on the right, overlying the atria and surrounding the aorta. Both fat pads are circled in red.

Chapter 2

MATERIALS AND METHODS

2.1 Animal Husbandry

Male Ross 708 broiler chickens (*Gallus gallus*) were obtained from Mountaire Hatchery(Millsboro, DE) and were raised according to the standards set by the University of Delaware Institutional Animal Care and Use Committee Guidelines [AACUC #(27) 03-12-14R] from day of hatch (DOH) until Day 42 (D42) post hatch, market age. At hatch they were placed in a house at 35˚C and the temperature was decreased to 25˚C over the following three weeks. Lighting was 23 hours light and 1 hour of dark. Standard Broiler feed and water were provided ad libitum. The food ratio met the standards set by the NRC (National Research Council, 1994).

2.2 Sample Pooling and Overall Experimental Design

Samples were taken from two different trials, Fall 2012 and 2013, to reach eight total samples of each adipose tissue. At least five subjects (birds) were required to be statistically powerful, identifying >75% of enriched genes at 20-30 million read sequence depth according to Schurch et al. (9), and there was not enough good quality RNA from a single trial to complete the analysis. These studies were performed with broiler chickens divided into two groups: control (thermoneutral) or heat stress, in which birds were subject to a cyclical pattern of heat stress. Only samples from the thermoneutral condition were used in this thesis.

2.3 Necropsy and Tissue Collection

The birds were euthanized at D42 by cervical dislocation, necropsied, and samples of abdominal and cardiac adipose tissue were flash frozen in liquid nitrogen and stored at -80˚C.

2.4 RNA Sequencing (RNA-Seq) Procedure

A workflow diagram describing the procedure is depicted in Figure 2. Total RNA extraction was performed on abdominal and cardiac adipose samples using the mirVana miRNA isolation kit with phenol (Carlsbad, CA) on 90 mg of adipose followed by DNase treatment using the Ambion DNA-free™ Kit DNase Treatment and Removal Reagents (Carlsbad, CA). The messenger RNA (mRNA) was then quality checked through fragment analysis at the Delaware Biotechnology Institute (DBI, Newark, DE) and quantified using the Qubit Fluorometer. Eight mRNA samples from each type of adipose tissue were made into complementary DNA (cDNA) libraries, using the Illumina Stranded RNAseq kit (San Diego, CA). The libraries were sequenced to a depth of 20-30 million mapped reads using the Illumina HiSeq 2500 sequencer at the DBI Core Sequencing Facility (Newark, DE). The sequence reads were then mapped to the chicken reference genome, Gallus Gallus ver4 (GalGal4), and run through an in house pipeline, fRNAkenseq, to generate gene expression levels in the form of fragments per kilobase of transcript per million mapped reads (FPKM) values. This normalizes the raw map counts to the length of the gene and the sequence depth of each library, giving a uniform comparison of expression for each gene in each library.

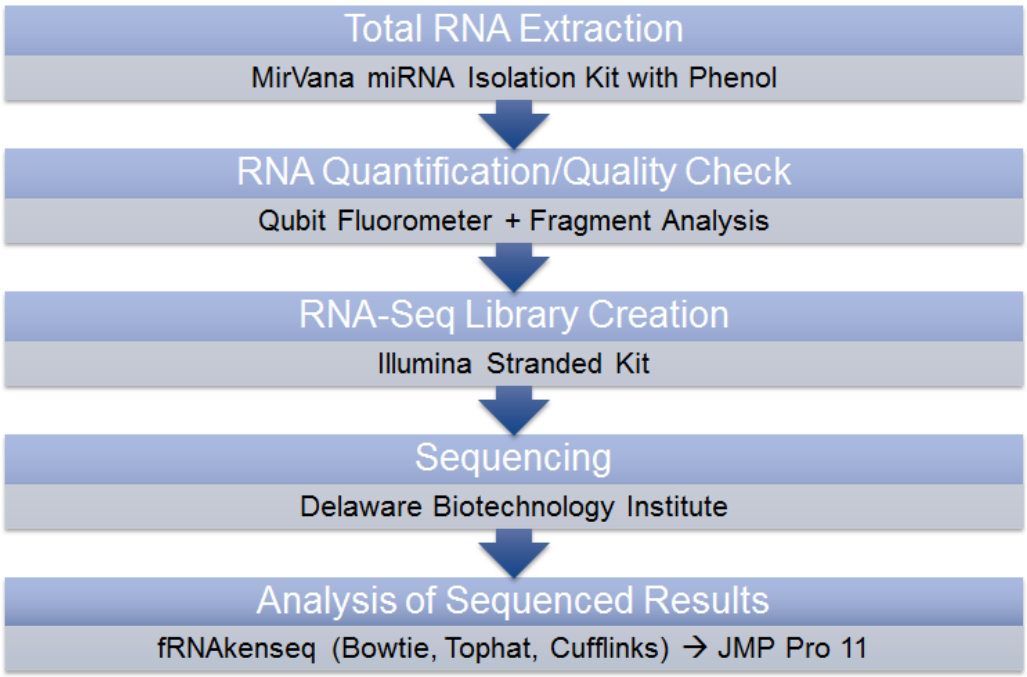

Figure 2: This figure is a workflow diagram of the RNA-Seq procedure. The details of this procedure can be found in the Materials and Methods section, subsection RNA Sequencing (RNA-Seq) Procedure.

2.5 Relative Tissue Expression (RTE) Analysis

The relative tissue expression analysis procedure was conducted as described by Bailey et al., 2009 (10). A workflow diagram describing the procedure is depicted in Figure 3. The goal of RTE is to determine the enriched genes that are unique to each type of adipose tissue in comparison to all other tissues (the rest of the body) of the chicken. The gene expression levels, or FPKM values, of each type of adipose were compared against other tissues including: pituitary, hypothalamus, liver, spleen, breast muscle, heart, pineal, retina, and spleen. This analysis was performed separately for both abdominal and cardiac adipose. First, the outliers were trimmed within the sample by taking the ratio of the maximum FPKM value to median FPKM

value for each gene in the adipose. The relative expression, or adipose enriched genes, were then identified by taking the ratio of maximum FPKM value in adipose to the median FPKM value in all other tissues. To normalize the distribution, a Log base 2 transformation was applied. These values were then subjected to a T-test and genes with P-values < 0.05 were considered to be enriched in adipose tissue.

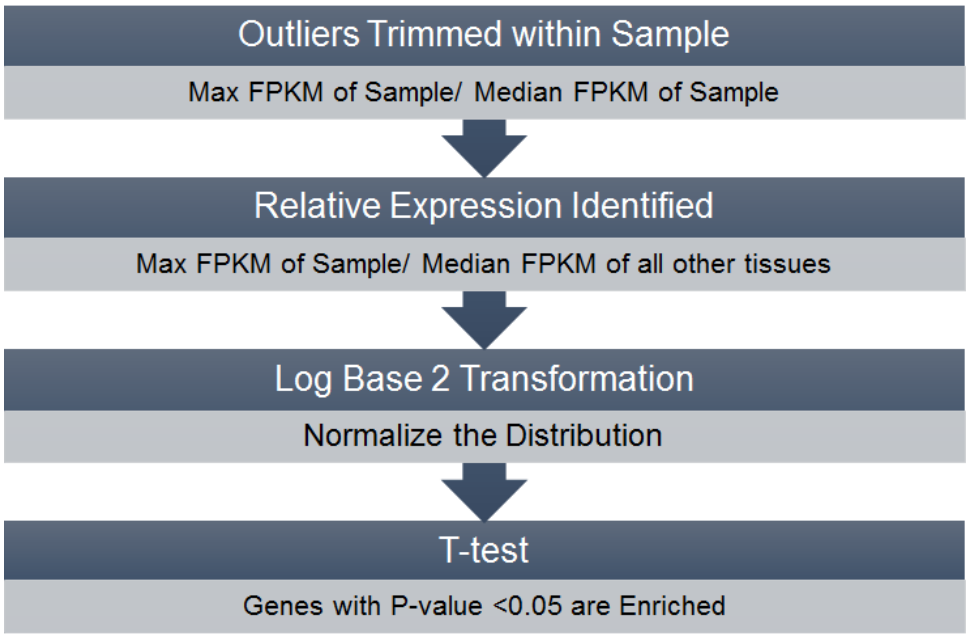

Figure 3: This figure is a workflow diagram of the relative tissue expression (RTE) analysis. The details of this procedure can be found in the Materials and Methods section, subsection Relative Tissue Expression (RTE) Analysis.

2.6 Bioinformatics Analysis

The enriched gene lists from the RTE analysis were then compared to each other to identify the overlapping genes using a Venn diagram, http://bioinformatics.psb.ugent.be/webtools/Venn/. The term "overlapping gene" identifies genes that were enriched in both the abdominal and cardiac adipose,

compared to all other tissues. The overlapping genes likely participate in functions common to both fat pads. Conversely, the term "unique" denotes genes only expressed by one type of fat. The gene lists were analyzed separately with the following procedure (Figure 4). Gene ontology (GO) terms were identified using AmiGO2 (11). GO terms are terms assigned to a gene by a consortium that are pulled from a hierarchy of biologically or functionally relevant terms. Enriched pathways were identified using PathRings (12). i-Terms, terms that are significantly enriched in the literature in a given gene in comparison to all genes, were identified through the text mining tool WebGIVI (13). Together, these different tools along with a literature search were used to identify pathways and regulatory functions of the enriched genes in each type of adipose tissue.

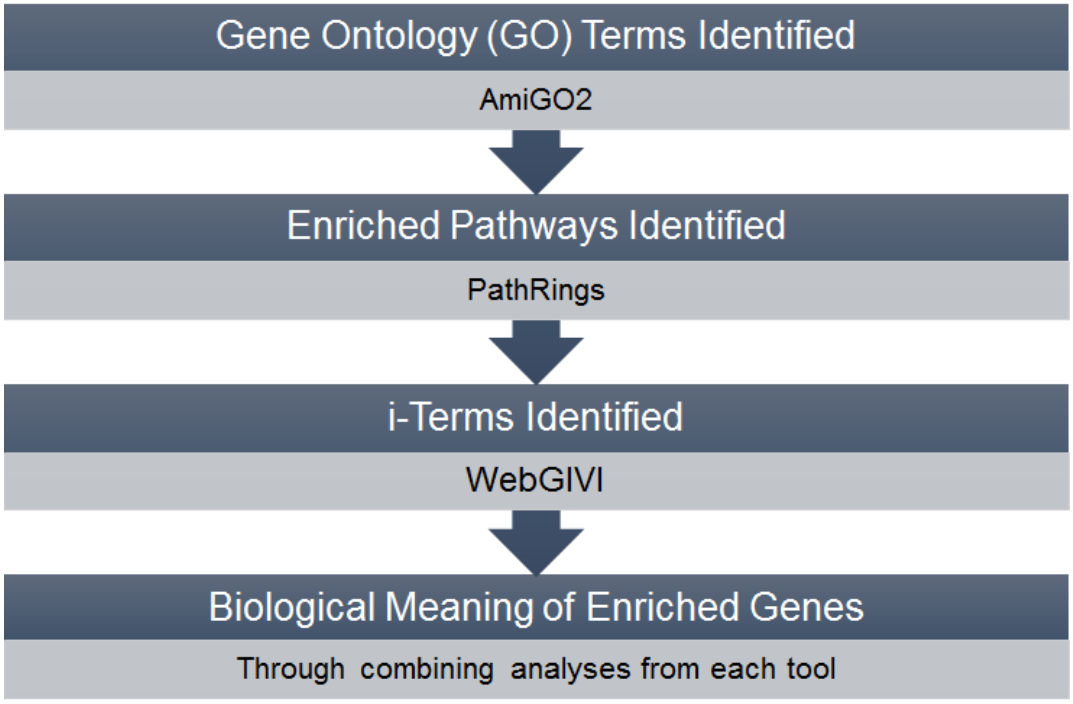

Figure 4: This figure is a workflow diagram of the bioinformatic tool analysis and how biological meaning is discovered from RNA-seq enriched gene lists. The details of this procedure can be found in the Materials and Methods section, subsection Bioinformatics Tool Analysis.

Chapter 3

RESULTS, ANALYSIS, AND DISCUSSION

The raw fastq sequence files have been deposited in the NCBI-GEO database and can be accessed at: https://www.ncbi.nlm.nih.gov/geo/query/acc.cgi?acc=GSE89643. After performing the RTE analysis, there were 202 overlapping genes (enriched in both abdominal and cardiac adipose tissue), 136 unique cardiac adipose genes, and 185 unique abdominal adipose genes (Figure 5).

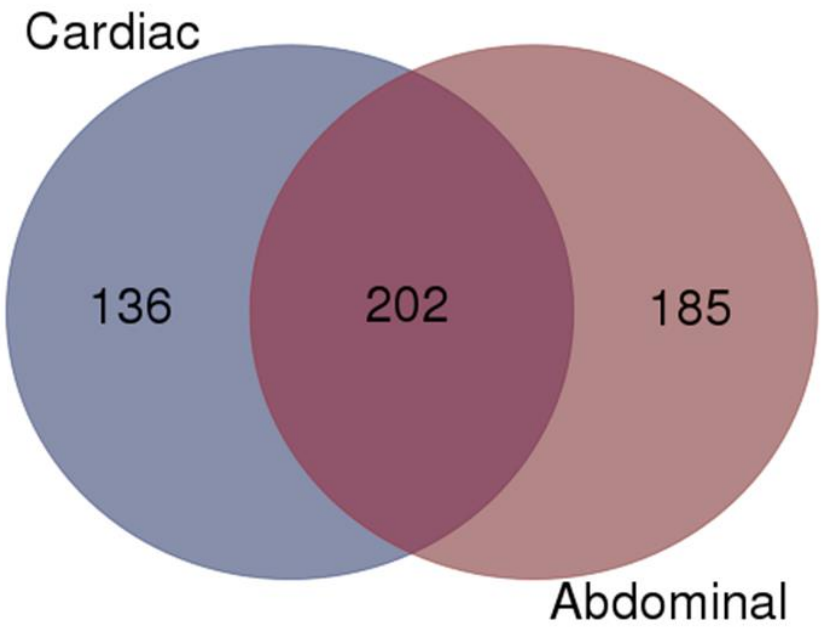

Figure 5: This figure shows the number of enriched genes, according to the RTE analysis or in comparison to the rest of the body, in the cardiac (blue) and abdominal adipose (mauve) tissue of the modern broiler chicken, along with the number of genes that overlap between the two anatomic sites (maroon).

The GO terms associated with the overlapping genes are typical of what would be predicted for adipose functions including: lipid storage, extracellular matrix organization, extracellular structure organization, angiotensin activated signaling pathway, regulation of body fluid levels, regulation of lipid storage, regulation of sequestering of triglycerides, lipid localization, developmental process, and regulation of inflammatory response (Table 1).

Table 1: This table displays 10 listed gene ontology (GO) terms associated with the Relative Tissue Expression (RTE) analysis for the overlapping enriched genes in both the abdominal and cardiac adipose tissue of the modern broiler chicken. The GO terms selected for display were significant based on p-value and deemed relevant or useful for analysis by the author.

Ontology Term	Genes in the Reference Genome	Tissue Specific Genes	Genes Expected By Chance	Fold Enrichment	P-Value
Lipid Storage	23	6	0.17	35.2	2.60E-08
Extracellular Matrix Organization	131	9	0.97	9.27	6.87E-07
Extracellular Structure Organization	132	9	0.98	9.2	7.31E-07

Angiotensin-Activated Signaling Pathway	14	4	0.1	38.56	4.23E-06
Regulation of Body Fluid Levels	173	9	1.28	7.02	6.49E-06
Regulation of Lipid Storage	25	4	0.19	21.59	4.04E-05
Regulation of Sequestering of Triglyceride	9	3	0.07	44.98	4.59E-05
Lipid Localization	338	11	2.5	4.39	4.67E-05
Developmental Process	3230	42	23.94	1.75	8.07E-05
Regulation of Inflammatory Response	142	7	1.05	6.65	9.96E-05

The GO terms associated with the cardiac adipose unique genes include: opsonization, heart development, pathway-restricted SMAD protein phosphorylation, regulation of peptidyl-serine phosphorylation of STAT protein, defense response to virus, humoral immune response, negative regulation of transmembrane receptor protein serine/threonine kinase signaling pathway, negative regulation of exo-alpha-sialidase activity, and cell proliferation involved in heart valve development (Table 2).

Table 2: Top 10 gene ontology (GO) terms associated with the Relative Tissue Expression (RTE) analysis for the enriched genes in the cardiac adipose tissue of the modern broiler chicken. The GO terms selected for display were significant based on p-value <0.05 and deemed biologically relevant by the author. The reference genome used was the chicken genome (*Gallus gallus*).

Ontology Term	Genes in the Reference Genome	Tissue Specific Genes	Genes Expected By Chance	Fold Enrichment	P-Value
Opsonization	3	2	0.01	>100	6.56E-05
Heart Development	482	7	1.33	5.25	3.65E-04
Pathway-restricted SMAD protein phosphorylation	13	2	0.04	55.63	6.21E-04

Regulation of Peptidyl-Serine Phosphorylation of STAT Protein	15	2	0.06	34.51	1.59E-03
Defense Response to Virus	61	3	0.24	12.73	1.76E-03
Humoral Immune Response	63	3	0.24	12.33	1.92E-03
Negative Regulation of Transmembrane Receptor Protein Serine/Threonine Kinase Signaling Pathway	75	3	0.29	10.35	3.14E-03
Negative Regulation of Exo-Alpha-Sialidase Activity	1	1	0	>100	3.86E-03
Cell Proliferation Involved in Heart Valve Development	1	1	0	>100	3.86E-03

The GO terms associated with the abdominal adipose unique genes include: cell adhesion, signal transduction, cytotoxic T cell differentiation, negative regulation of heterotypic cell-cell adhesion, cell communication, positive regulation of phospholipid biosynthetic process, regulation of secondary metabolite biosynthetic process, T cell mediated immunity, positive regulation of lipid biosynthetic process, and regulation of Interleukin-8 production (Table 3). A summary of the results of what is important for each type of adipose tissue is depicted in Figure 6.

Table 3: Top ten (10) gene ontology (GO) terms associated with the Relative Tissue Expression (RTE) analysis for the enriched genes in the abdominal adipose tissue of the modern broiler chicken. The GO terms selected for display were significant based on p-value <0.05 and deemed biologically relevant by the author. The reference genome used was the chicken genome (*Gallus gallus*).

Ontology Term	Genes in the Reference Genome	Tissue Specific Genes	Genes Expected By Chance	Fold Enrichment	P-Value
Cell Adhesion	580	16	3.75	4.27	1.03E-06
Signal Transduction	2741	34	17.71	1.92	7.11E-05
Cytotoxic T Cell Differentiation	14	3	0.09	33.17	1.12E-04

Negative Regulation of Heterotypic Cell-Cell Adhesion	3	2	0.02	>100	1.84E-04
Cell Communication	3009	35	19.44	1.8	1.99E-04
Positive Regulation of Phospholipid Biosynthetic Process	4	2	0.03	77.4	3.25E-04
Regulation of Secondary Metabolite Biosynthetic Process	5	2	0.03	61.92	5.06E-04

T Cell Mediated Immunity	25	3	0.16	18.58	6.06E-04
Positive Regulation of Lipid Biosynthetic Process	25	3	0.16	18.58	6.06E-04
Regulation of Interleukin-8 Production	26	3	0.17	17.86	6.79E-04

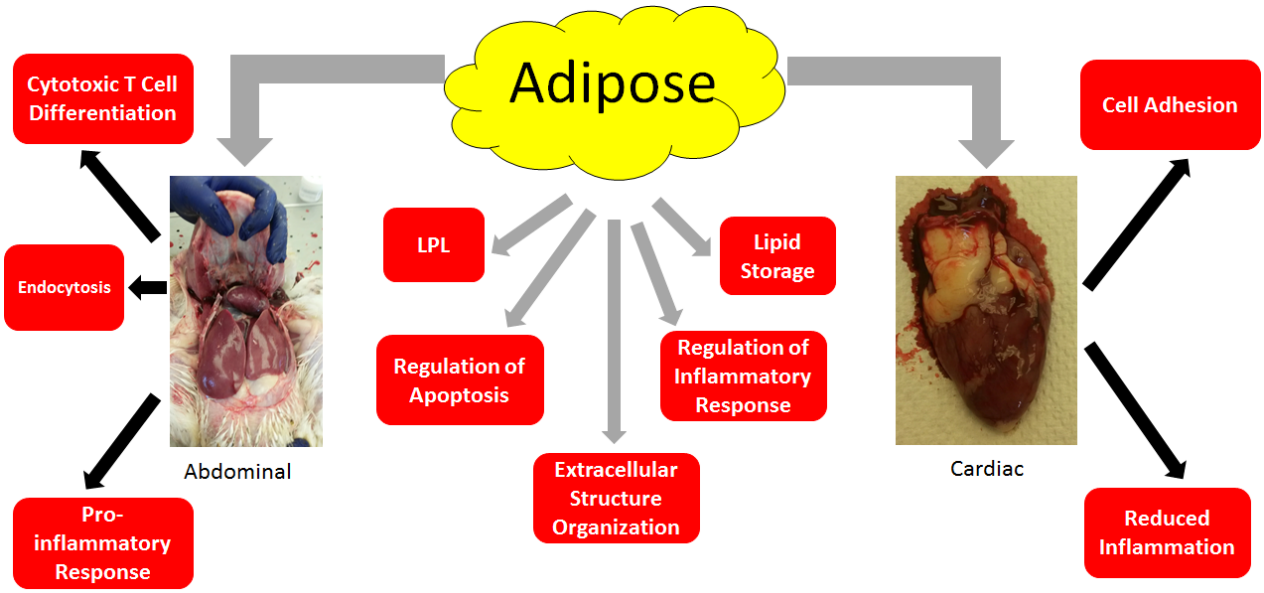

Figure 6: A summary of the results of the RNA-seq analysis, highlighting pathways common across adipose depots, overlapping, as well as pathways unique to each type of adipose, abdominal or cardiac, tissue in the modern broiler chicken.

3.1 Energy Homeostasis

When the overlapping enriched genes were examined in the PathRings program the six genes were identified that were categorized into the pathway "Transcriptional Regulation of White Adipocyte Differentiation" (Figures 7-8 and Table 4).

Developmental Biology

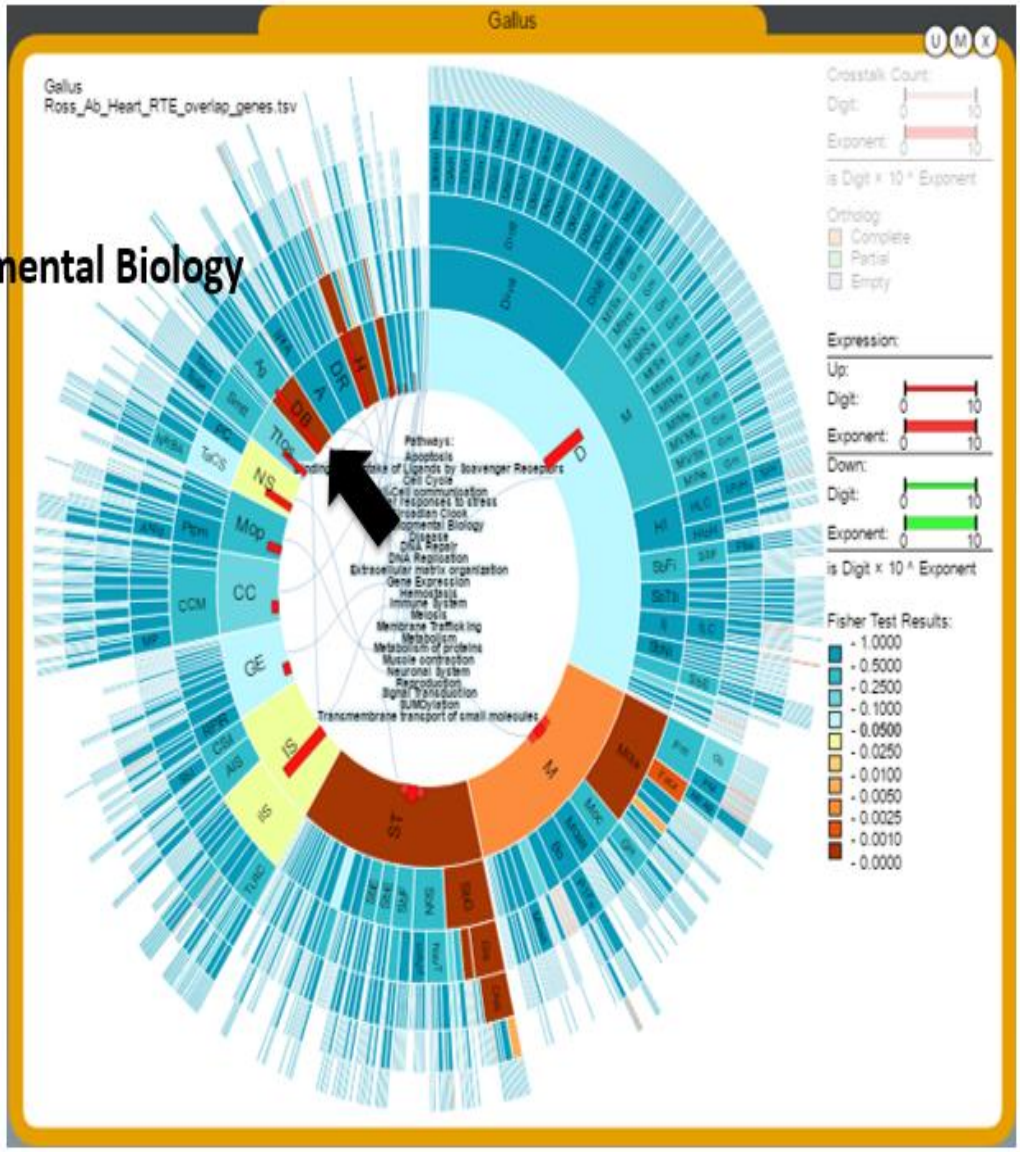

Figure 7: This figure displays the significant pathways found by the PathRings program using a Fisher's exact test based on the expression levels of each gene in the chicken, specifically for the RTE analysis of the overlapping enriched genes, in both the cardiac and abdominal adipose tissue of the modern broiler chicken. The red color indicates significance, as shown in the key. Here the Developmental Biology pathway is seen to be significant, indicated by the arrow. The red bars represent the genes enriched in each pathway; red bars are only displayed because the green bars, which indicated down regulation, would indicate genes in pathways that are enriched in every other tissue and different lines of chicken, which is not the focus of this paper.

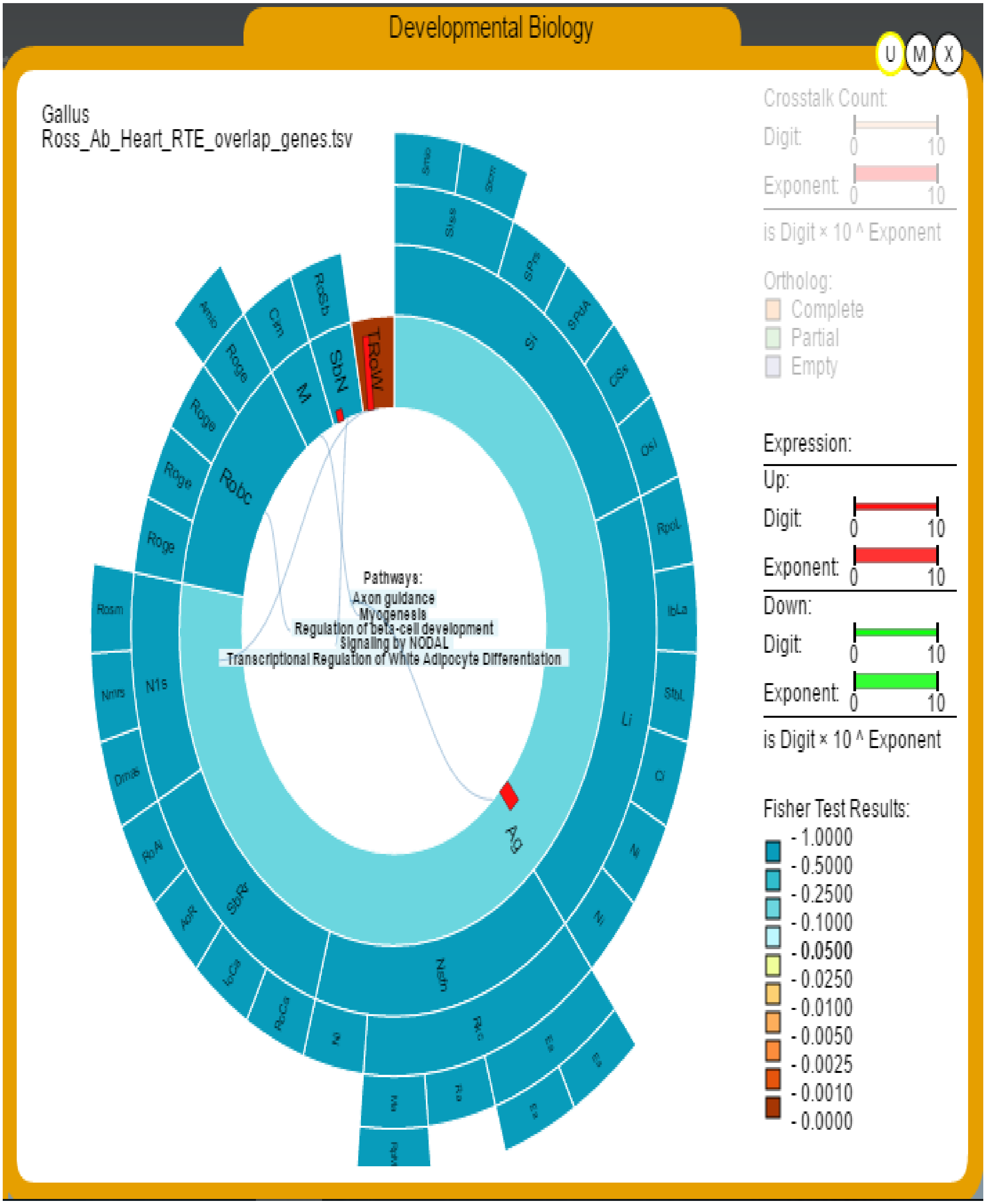
Developmental Biology
U
M
X
Gallus
Ross_Ab_Heart_RTE_overlap_genes.tsv
Crosstalk Count:
Digit:
Exponent:
is Digit × 10 ^ Exponent
Ortholog:
Complete
Partial
Empty
Expression:
Up:
Digit:
Exponent:
Down:
Digit:
Exponent:
is Digit × 10 ^ Exponent
Fisher Test Results:
- 1.0000
- 0.5000
- 0.2500
- 0.1000
- 0.0500
- 0.0250
- 0.0100
- 0.0050
- 0.0025
- 0.0010
- 0.0000
Pathways:
Axon guidance
Myogenesis
Regulation of beta-cell development
Signaling by NODAL
Transcriptional Regulation of White Adipocyte Differentiation
TRoWA
SbN
M
Robc
N1s
Li
Ag
Nsfn

Figure 8: Displays a closer look at the significant Developmental Biology pathway, where the Transcriptional Regulation of White Adipocyte Differentiation pathway is seen to be significant. The red color indicates significance, as shown in the key. The red bars represent the genes enriched in each pathway; red bars are only displayed because the green bars, which indicated down regulation, would indicate genes in pathways that are enriched in every other tissue and different lines of chicken, which is not the focus of this paper.

Table 4: This table displays the six genes identified in the Transcriptional Regulation of White Adipocyte Differentiation pathway with LPL being a rate limiting gene.

Gene Name	symbol	gene_id	ratio
collagen type VI alpha 2 chain	COL6A2	396292	5.15298
netrin 1	NTN1	396389	5.05594
activin A receptor type 1C	ACVR1C	424325	8.86332
early B-cell factor 1	EBF1	395512	5.34392
peroxisome proliferator activated receptor gamma	PPARG	373928	6.42162
fatty acid binding protein 4	FABP4	374165	13.05472
lipoprotein lipase	LPL	396219	7.44716
CCAAT/enhancer binding protein alpha	CEBPA	427549	5.67663
CD36 molecule	CD36	417730	6.91768

Lipoprotein Lipase (LPL) is the rate limiting enzyme in the hydrolysis of triglycerides and transport of lipoproteins via receptor mediated endocytosis. The enrichment of this enzyme in both fat pads is consistent with the essential role of LPL in fat uptake and regulation of circulating lipoproteins. Another overlapping gene, CCAAT/enhancer binding protein alpha (CEBPA) is a transcription factor that functions in regulation of the cell cycle. Peroxisome proliferator activated receptor gamma (PPARG) is also an enriched overlapping gene, critical to the differentiation of adipocytes from stem cells.

Further investigation identified a feed forward loop between PPARG and CEBPA that appears to be present in mature adipocytes (14). Figure 9 shows the predicted pathway of how these enriched genes are related to one another in the formation and maintenance of the adipocyte phenotype. Fatty Acid Binding Protein 4 (FABP4) joins and consolidates long-chain fatty acids in the cytoplasm. FABP4 inhibits PPARG at the protein level (15). An increase in PPARG leads to an increase in CEBPA through the feed forward loop (14). Elevated CEBPA then increases the transcription of genes critical to adipocyte function including, Cluster of Differentiation 36 molecule (CD36) and LPL which control the uptake of low density lipoproteins (LDL) and adipogenesis. However, instead of seeing a decrease FABP4 expression, it was enriched in both cardiac and abdominal adipose.

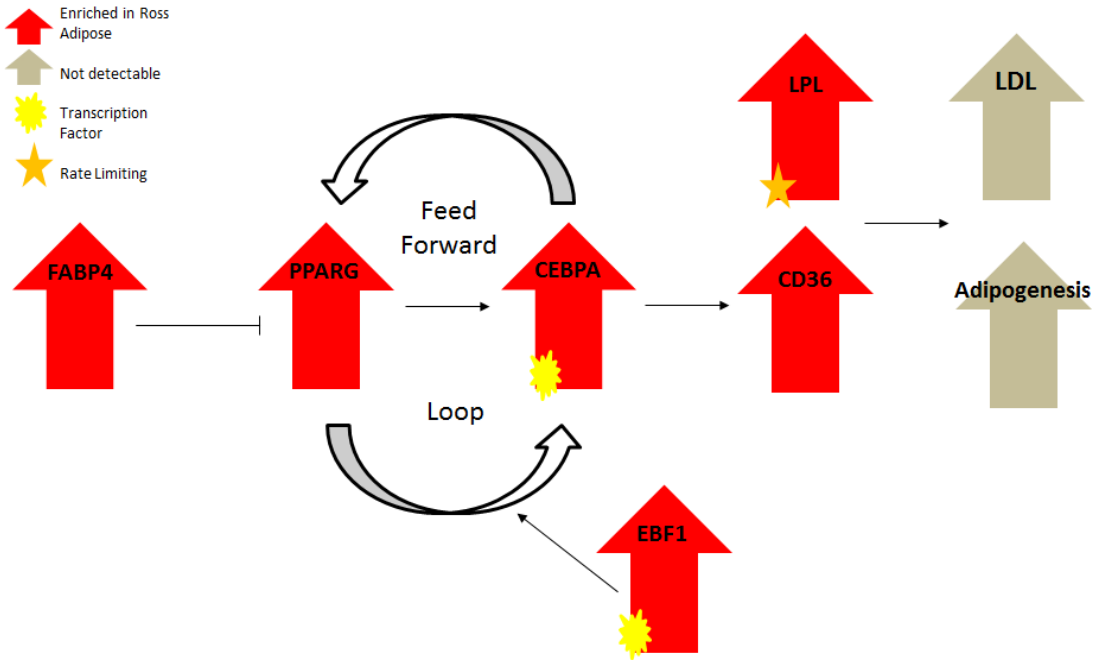

Figure 9: This figure displays the hypothesized relationship between the overlapping RTE enriched genes in both the cardiac and abdominal adipose tissue in the modern broiler chicken that were indicated to be involved in the Transcriptional Regulation of White Adipocyte Differentiation pathway. A feed forward loop that exists between CEBPA and PPARG along with the rest of the pathway that ultimately leads to an increase in adipogenesis and is likely to be used to maintain the adipocyte phenotype. It is important to note that the data contradicts the inverse relationship between FABP4 and PPARG. Another feed forward loop between EBF1 and CEBPA that could be increasing CEBPA expression levels to the point where it makes up for FABP4 not being depressed. Overall this pathway is hypothesized to maintain energy/lipid homeostasis, including both lipolysis and lipid storage. While this data is a good indication at what is going on in adipose tissue, another important thing to note is we are looking at the mRNA expression and this cannot be directly viewed as what is going on at the protein level.

Early B-cell Factor 1 (EBF1) was also an overlapping gene and functions in regulating inflammation, metabolism, and signal transduction in adipose tissue (16).

Elevated EBF1 leads to an increase in the transcription of CEBPA by activation of its promoter (17). An increase in CEBPA then leads to an increase in the heterodimer CCAAT/enhancer binding protein delta (CEBPD), which, along with CCAAT/enhancer binding protein beta (CEBPB) comprise a feed forward loop, increasing EBF1 (17). CEBPD is not found in chickens however. Expression of EBF1 could be increasing the CEBPA to offset the elevated FABP4 levels. The increase in CEBPA, would then explain the enrichment of PPARG through the feed forward loop. Additionally, EBF1 activates the promoter for PPARG (17).

3.2 Extracellular Matrix Organization

Another pathway that was significant in PathRings for the overlapping genes was the Extracellular Matrix Organization (ECMO) pathway. There were 10 genes enriched in the ECMO pathway (Table 5).

Table 5: This table displays the 10 genes identified in the Extracellular Matrix Organization pathway for the overlapping enriched genes, in both the abdominal and cardiac adipose tissue in the modern broiler chicken, with no rate limiting genes being identified.

Gene Name	symbol	gene_id	Ratio
collagen type XX alpha 1 chain	COL20A1	419243	6.21094
collagen type VI alpha 2 chain	COL6A2	396292	5.15298
collagen type XXVIII alpha 1 chain	COL28A1	420576	6.6349
ADAM metallopeptidase with thrombospondin type 1 motif 2	ADAMTS2	416291	6.03273

procollagen C-endopeptidase enhancer 2	PCOLCE2	429124	5.2849
lysyl oxidase	LOX	396474	5.4804
microfibrillar associated protein 5	MFAP5	418256	5.46337
Asporin	ASPN	415954	6.20753
cartilage oligomeric matrix protein	COMP	420120	7.37145
ADAM metallopeptidase with thrombospondin type 1 motif 5	ADAMTS5	427971	5.77218

Transforming growth factor beta (TGFB) regulates the formation of key components of the extracellular matrix (ECM). It is important to note that while TGFB is not enriched in either adipose tissue, activin a receptor type 1C (ACVR1) is a member of the TGFB family and is an enriched overlapping gene. TGFB increases the expression of lysyl oxidase (LOX), whose protein product is responsible for linking collagen and elastin to form elastin fibers (18), and is an overlapping gene (19). EGF containing fibulin like extracellular matrix protein 2 (EFEMP2), which is involved in the formation of elastin fibers, links LOX to tropoelastin, the core of elastin fibers, allowing it to cleave tropoelastin, forming elastin (20–22). Fibrillin 1 (FBN1), a glycoprotein that is part of the extracellular matrix microfibrils and helps support the structure of the cell and is unique to the cardiac adipose tissue, co-localizes with microfibrillar associated protein 5 (MFAP5), a glycoprotein that attaches to the microfibrils of the ECM and an overlapping gene, leading to the release elastin globules (21,23).

TGFB also aids in the maturation of collagen through two different pathways. TGFB elevates ADAM metallopeptidase with thrombospondin type 1 motif 2 (ADAMTS2) (24, 25), an overlapping gene responsible for cleaving procollagens (24, 25). Cleavage allows for formation of mature collagen and its incorporation into the elastin fibers of the ECM. In addition to its impact on fiber formation, LOX increases the collagen type I (COL1) and collagen 3 (COL3) by aiding in the maturation process (26). MFAP5 also stabilizes procollagen 1 and COL1 increases the amount of cartilage oligomeric matrix protein (COMP) (27, 28). COMP helps regulate the production of collagen type II (COL2) and links COL2 with collagen type IX (COL9) (29, 30). In addition, heparan sulfate proteoglycan 2 (HSPG2), which is associated with ECM binding and function, is unique to cardiac adipose and binds to collagen type IV (COL4) (31). Finally, collagen type XXVIII alpha 1 chain (COL28A1) and collagen type VI alpha 2 chain (COL6A2) are overlapping genes. COL6A2 has affinity for ECM proteins and may aid in the binding of MFAP5 and/or TGFB.

Figure 10 illustrates how the elastin component and the collagen component, both regulated by TGFB, come together to form the ECM. The elastin fiber is composed of an inner core of tropoelastin, surrounded by an outer layer of fibrillins, including FBN1, and microfibrillar associated proteins, including MFAP5 (21). An increase in tropoelastin leads to an increase/regulation of FBN1 and other fibrillins, forming both the core to the outer layer of the elastin fiber (32). LOX links the elastin fibers and collagen together to form the ECM (33). All of the components of the ECM and these enriched genes lead to an ultimate increase in integrin binding, cell adhesion, wound healing, ECM integrity, and elasticity. In mammals, HSPG2 increases integrin binding in the ECM which increases cell adhesion, along with

aiding in wound healing (33, 34). FBN1 also, was shown to play a role in the process of cell adhesion (35). The specific, binding of the collagen and elastin fiber components of the ECM was shown to increase the strength and integrity of the ECM (33). Finally, elasticity is also increased with increased tropoelastin, LOX, and FBN1 (36, 37).

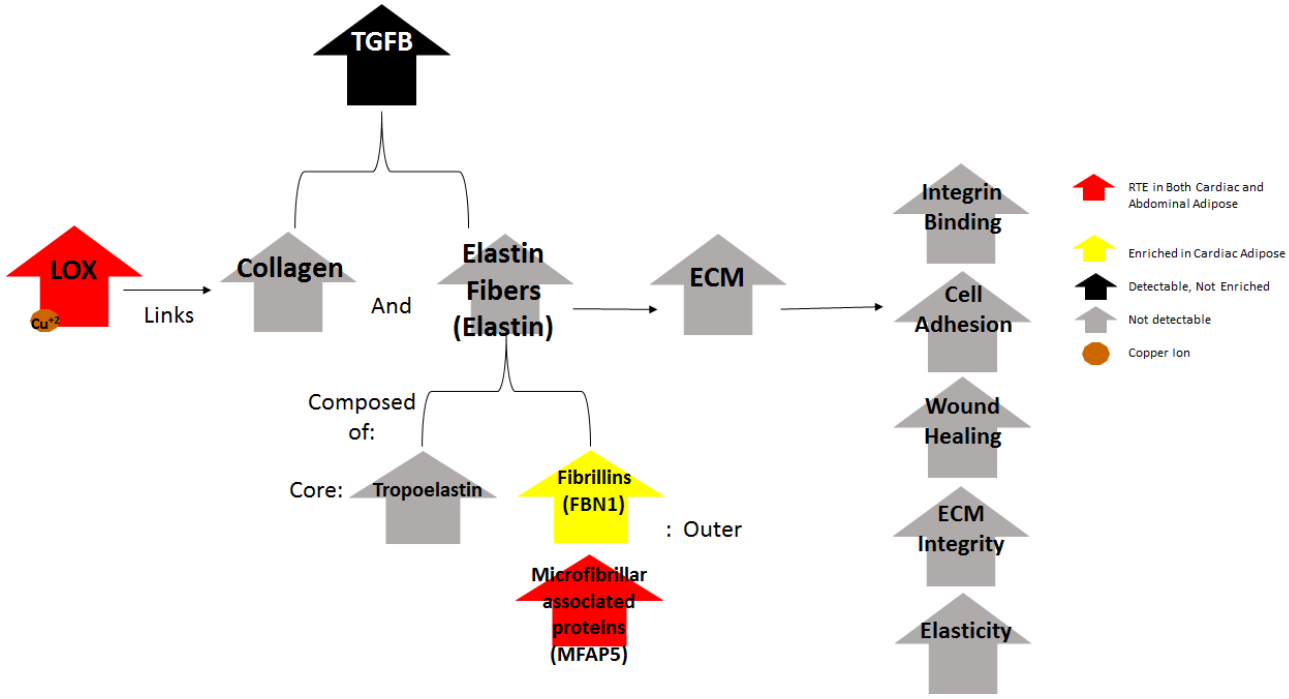

Figure 10: This figure displays the role that TGFB plays in the formation of the ECM along with the total effects of the enriched genes on the ECM. The ultimate goal being to provide stability in the structure of the ECM. While this data is a good indication at what is going on in adipose tissue, another important thing to note is we are looking at the mRNA expression and this cannot be directly viewed as what is going on at the protein level.

TGFB appears to be the main regulator in the creation of both elastin and collagen, which together form the ECM. TGFB however, is itself regulated by multiple gene products, some of which are overlapping gene products and others that are unique to the cardiac adipose (Table 6 and Figure 11). MFAP5 was shown to increase the mitogen-activated protein kinase 1 (MAPK1) pathway and proliferation; MAPK1 activation was associated with the levels of TGFB captured in the ECM (38, 39). TGFB and MAPK1 then go onto induce the SMAD2/3 pathway which leads to a halt in the cell cycle and promotes ECM growth (38, 40). This suggests that MFAP5 releases TGFB from the ECM through proteinase activity, allowing for the activation of the SMAD2/3 pathway, increasing growth of the ECM. In addition, in a mouse model, in the presence of ADAMTS5, TGFB1 stimulation led to the activation of the SMAD family member 2/3 (SMAD2/3) (41) and ECM growth (40). However, there were also several genes enriched that inhibit TGFB release from the ECM. One example being, asporin (ASPN), a cartilage ECM protein that binds to collagen and calcium and inhibits TGFB and overlapping gene (42, 43). A negative feedback loop is present with SMAD3 increasing the amount of ASPN, which then goes on to inhibit TGFB (44). TGFB is also inhibited by LOX (45). LOXL4, unique to cardiac adipose, was also suggested to be increased by TGFB and then form a negative feedback loop to inhibit TGFB (46). Finally, FBN1 inhibits the TGFB levels by sequestering it within the ECM and decreasing further signaling (47).

Table 6: This table displays the 6 genes linked to extracellular matrix organization that regulate TGFB. Depending on how TGFB is regulated by certain genes determines its location in relation to the ECM. The overlapping enriched genes, in both the abdominal and cardiac adipose tissue in the modern broiler chicken, are indicated in red and the cardiac adipose unique genes are indicated in yellow.

Gene Name	Gene Symbol	Enrichment	Effect on TGFB	Where TGFB is in relation to the ECM
microfibrillar associated protein 5	MFAP5	Overlapping	Promotes	Released from the ECM
ADAM metallopeptidase with thrombospondin type 1 motif 5	ADAMTS5	Overlapping	Promotes	Released from the ECM
Asporin	ASPN	Overlapping	Inhibits	Sequestered in the ECM
lysyl oxidase	LOX	Overlapping	Inhibits	Sequestered in the ECM
fibrillin 1	FBN1	Cardiac Adipose	Inhibits	Sequestered in the ECM
lysyl oxidase like 4	LOXL4	Cardiac Adipose	Inhibits	Sequestered in the ECM

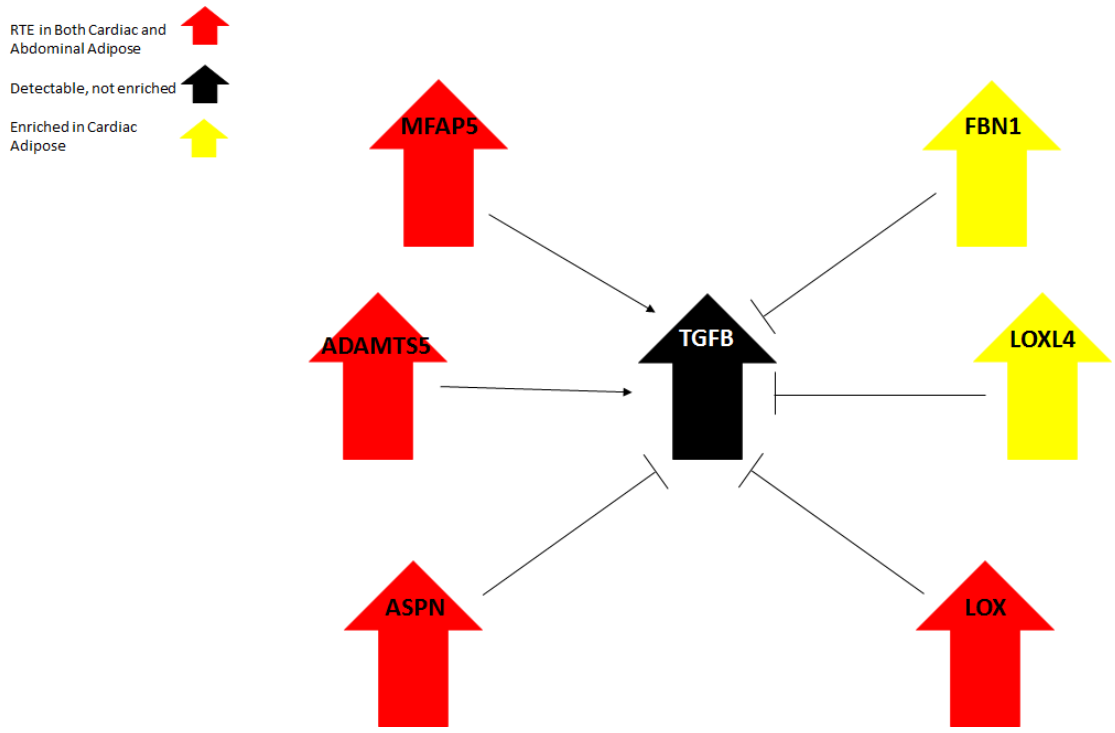

Figure 11: This figure displays the 6 genes linked to extracellular matrix organization that regulate TGFB, through either promotion or inhibition. The overlapping enriched genes, in both the abdominal and cardiac adipose tissue in the modern broiler chicken, are indicated in red and the cardiac adipose unique genes are indicated in yellow.

The overall trend that can be seen is that if TGFB is released from the ECM, it promotes Smad signaling, and enhances ECM growth. However, if TGFB is inhibited it remains sequestered in the ECM, unable to initiate Smad signaling and ECM growth. It would thus be hypothesized that since there are more inhibitors of TGFB in the cardiac adipose, the cardiac adipose has a more stable ECM, in comparison to the abdominal adipose. This could potentially be explained due to the fact that it is not the primary lipid depot; more lipids are leaving the abdominal adipose, degrading the ECM more, increasing the ECM growth to replace the damage done by lipid transport.

3.3 Aorta Regulation

Some of the enriched genes that were involved in the regulation of the ECM were also found to regulate cardiac function. A study in mice showed that a mutant version of FBN1, a cardiac unique gene, led to a decrease in elasticity and increase in stiffness in the aorta along with decreased overall heart function (48). LOX, an overlapping gene, was suggested to influence vascular remodeling (49). Additionally, an increase in tropoelastin and LOX, leads to an increase in nitric oxide (NO), which then leads to increase elasticity in the aorta (36), along with vasodilation. Perhaps, expression of FBN1 and LOX in the cardiac adipose tissue serves not only to function in the ECM integrity in the adipose tissue but could also be aiding the maintenance of the vasculature, particularly, the aorta.

HSPG2, another cardiac fat unique gene, was shown to induce the adhesion of smooth muscle cells (50). This could affect the localization of the cardiac adipose tissue, since mesenchymal stem cells arrive from the vasculature (51) and the cardiac fat pad surrounds the vasculature, especially the aorta, which is smooth muscle. HSPG is also known to play a role in the cardiovascular functioning, specifically in the regulation of the ECM, smooth muscle activation, antithrombic activity, vascular permeability, and insulin sensitivity (52). In addition, HSPG2 was also shown to be involved in angiogenesis, cell adhesion, and differentiation/ proliferation (53). Figure 12 depicts a summary of the effects of the enriched adipose genes on the vasculature, specifically the aorta.

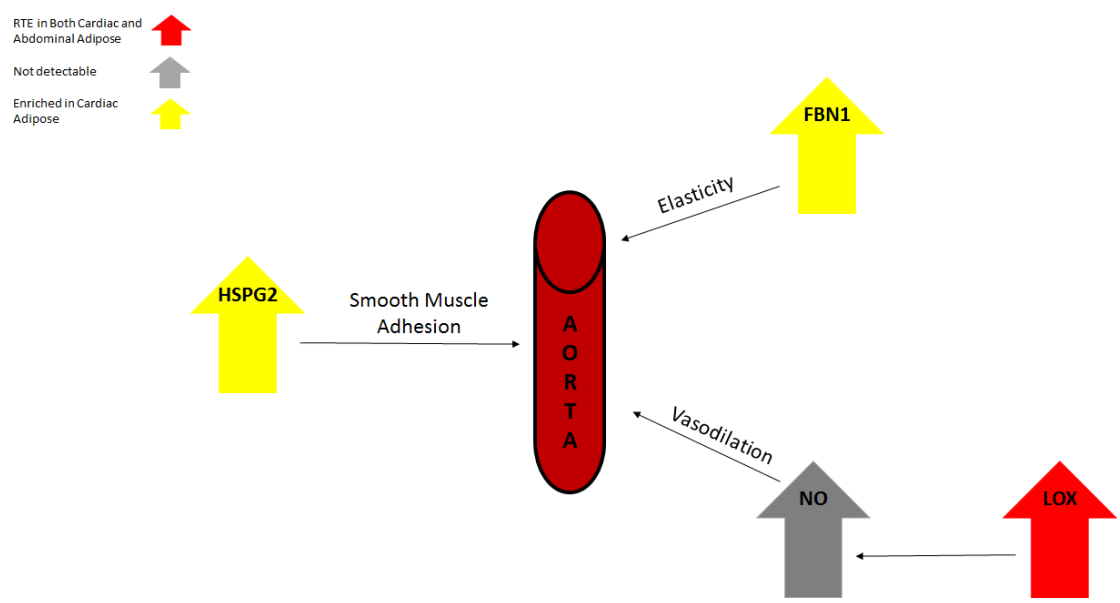

Figure 12: This figure displays the enriched adipose genes and the affects that they could have on the aorta. The overlapping enriched genes, in both the abdominal and cardiac adipose tissue in the modern broiler chicken, are indicated in red and the cardiac adipose unique genes are indicated in yellow.

3.4 Immune Functioning

GO analysis indicated that the main differences between the cardiac and abdominal adipose tissue centered on differences in immune functions, with abdominal adipose being associated with T-cell functions. The overlapping genes that were associated with the Immune System pathway in PathRings are listed in Table 7. The genes that are unique to the cardiac adipose and associated with the Immune System pathway are listed in Table 8. The genes that are unique to the abdominal adipose and associated with the Immune System pathway are listed in Table 9.

Table 7: This table displays the 7 genes identified in the Immune System pathway for the overlapping enriched genes, in both the abdominal and cardiac adipose tissue in the modern broiler chicken, with no rate limiting genes being identified.

Gene Name	Symbol	gene_id	ratio
CD36 molecule	CD36	417730	6.91768
CD14 molecule	CD14	100194427	5.3491
ADP-ribosyltransferase 1	ART1	429485	5.73508
protein kinase cAMP-dependent type II regulatory subunit beta	PRKAR2B	769420	5.68868
ubiquitin specific peptidase 18	USP18	418167	5.84525
hepatocyte growth factor	HGF	395941	5.976
fibroblast growth factor 7	FGF7	415439	7.62155

Table 8: This table displays the 3 genes identified in the Immune System pathway for the cardiac adipose unique genes, in the modern broiler chicken, with no rate limiting genes being identified.

Gene Name	symbol	gene_id	ratio
complement C7	C7	427187	8.40924
MX dynamin like GTPase 1	MX1	395313	7.49352

fibroblast growth factor 16	FGF16	422330	7.0071

Table 9: This table displays the 5 genes identified in the Immune System pathway for the abdominal adipose unique genes, in the modern broiler chicken, with no rate limiting genes being identified.

Gene Name	Symbol	gene_id	ratio
vascular cell adhesion molecule 1	VCAM1	424467	2.45726
CD8a molecule	CD8A	403158	2.68797
Fos proto-oncogene, AP-1 transcription factor subunit	FOS	396512	2.64301
early growth response 1	EGR1	373931	2.56279
colony stimulating factor 2 receptor beta common subunit	CSF2RB	771315	2.29024

Figure 13 highlights the response to a gram negative bacterial infection through recognition of Lipopolysaccharide (LPS). Cysteine rich secretory protein LCCL domain containing 2 (CRISPLD2), which is secreted by natural killer (NK) cells, T cells, and monocytes and is unique to the cardiac adipose, and CD14 molecule (CD14), a macrophage surface antigen and overlapping gene, compete to bind LPS, a component of gram negative bacterial membranes (54). CRISPLD2 leads to a decrease in interleukin 6 (IL6), traditionally an inflammatory cytokine although there are instances where it decreases inflammation, by preventing its binding to LPS (54, 55). CD14 regulates inflammatory responses, when stimulated by LPS through the production of cytokines (56). The cytokines involved in the inflammatory response

that are enriched are as follows. Interleukin 18 receptor accessory protein (IL18RAP), part of the receptor for interleukin 18 (IL18), an inflammatory cytokine, and interleukin 4 induced 1 (IL4I1), a gene product that is induced by interleukin 4 (IL4), a cytokine that has both pro and anti-inflammatory effects (55), are unique to the cardiac adipose tissue. IL4 will be considered to be enriched in the cardiac adipose due to the fact that the IL4I1, which is enriched in the cardiac adipose, expression is induced by IL4. Interleukin 12B (IL12B), a subunit of the inflammatory cytokine that acts on T and NK cells, interleukin 12 receptor subunit beta 2 (IL12RB2), a subunit of the receptor for the inflammatory cytokine IL12, and colony stimulating factor 2 receptor beta common subunit (CSF2RB), a receptor subunit common to the receptors for interleukin 3 (IL3), colony stimulating factor 2 (CSF2), and interleukin 5 (IL5), are unique to the abdominal adipose tissue. When joined to interleukin 12 receptor subunit beta 1 (IL12RB1), IL12RB2, the less common subunit, allows IL12 to bond, triggering an immune response and the production of interferon gamma (IFNG), which promotes T cell differentiation (57). In the context of this pathway it would be hypothesized that there is regulation and dampening of inflammation in the cardiac adipose, possibly due to the fact that it is so close to the heart and inflammation could drastically affect cardiac functioning. While, the abdominal adipose appears to be slightly more pro-inflammatory based on the enrichment of IL12RB2, indicating that the inflammatory response caused by IL12 is easily stimulated.

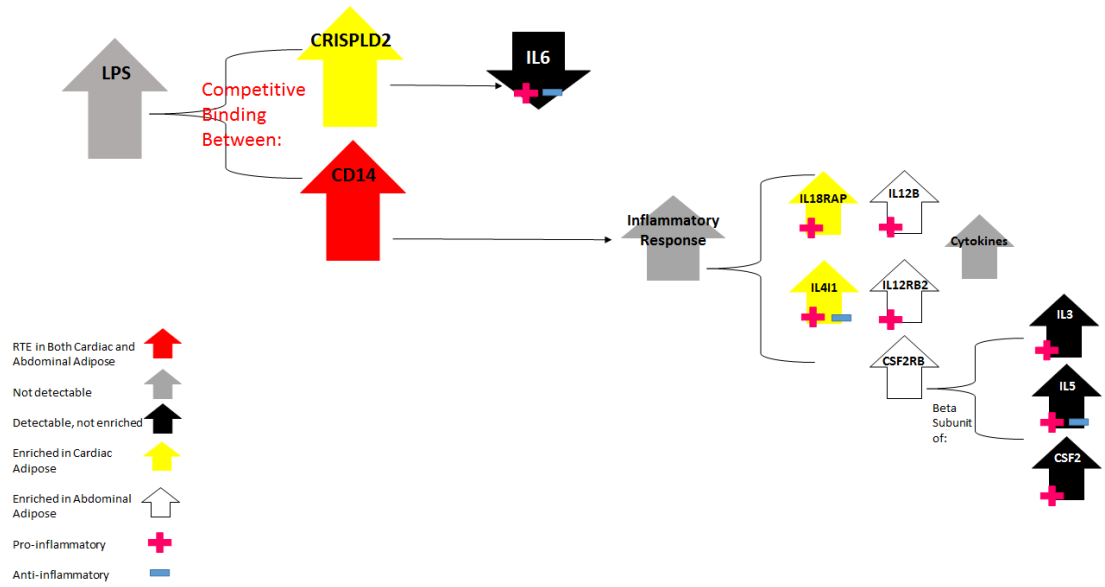

Figure 13: This figure displays the inflammatory response elicited mainly by CD14 molecule (CD14) to LPS, indicating a gram negative bacterial infection. The genes enriched in cardiac adipose, abdominal adipose, and/or both are indicated in yellow, white, and red respectively. The plus signs indicate pro-inflammatory cytokines and the minus signs indicated anti-inflammatory cytokines. While this data is a good indication at what is going on in adipose tissue, another important thing to note is we are looking at the mRNA expression and this cannot be directly viewed as what is going on at the protein level.

The GO term cytotoxic T cell differentiation was also assigned to the abdominal adipose unique genes; it is interesting that the main role that T cells play in adipose tissue is associated with initiation of inflammation (7). It should also be noted that there are three types of T cells, CD4, CD8, and NK cells (58). CD8A T cells secrete inflammatory cytokines (7) and CD8A was shown to be enriched in the abdominal adipose.

Figure 14 depicts the specific role that CD14 plays in the polarization of T lymphocytes and highlights the components of T helper type 1 (Th1) and T helper

type 2 (Th2) cells, subtypes of CD4 T cells (7). Th1 cells help eliminate intracellular pathogens, activate macrophages, and are characterized by the secretion of interferon gamma (IFNG), an inflammatory cytokine (59, 57). IFNG further enhances the Th1 phenotype by inhibiting Th2 and T helper type 17 (Th17) differentiation and activation of NK and CD8 cells (59). IL12 receptors are also a major component of Th1 cells (59). IL12RB2 is enriched in the abdominal adipose tissue. Th2 cells protect against parasitic worms and extracellular parasites, cause B cells to switch to the immunoglobulin E (IgE) class, activate eosinophils, mast cells, and basophils, cause mucus production, activate macrophages, enhance barrier function, and are characterized by IL4, IL5, and interleukin 13 (IL13), classically defined as anti-inflammatory cytokines (59). Interleukin 9 (IL9) is also a cytokine secreted from Th2 cells (60). IL4 initiates and propagates Th2 differentiation and inhibits Th1 differentiation along with IL13 (59). It is interesting that natural helper cells were discovered in adipose and are a major source of IL4 along with basophils, mast cells, and NK cells (59). IL4I1 is enriched in the cardiac adipose tissue. As stated before, endotoxin and LPS induce an antigen response by CD14 (61). CD14 polarizes T lymphocytes, which are present in adipose tissue in mice and humans (62), into Th1 and Th2 cells (61).

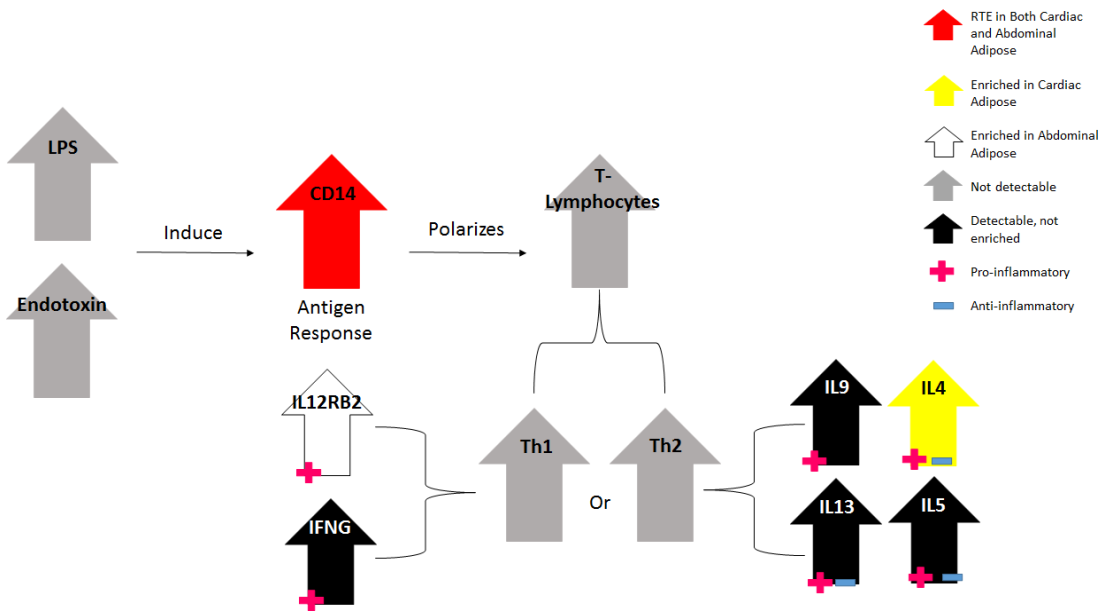

Figure 14: This figure displays the polarization of T-lymphocytes elicited mainly by CD14 molecule (CD14), in response to LPS. The types of cytokines and receptors associated with each type of T cell are depicted. The genes enriched in cardiac adipose, abdominal adipose, and/or both are indicated in yellow, white, and red respectively. The plus signs indicate pro-inflammatory cytokines and the minus signs indicated anti-inflammatory cytokines. While this data is a good indication at what is going on in adipose tissue, another important thing to note is we are looking at the mRNA expression and this cannot be directly viewed as what is going on at the protein level.

Figure 15 demonstrates the effects of how IFNG influences Th1 and Th2 differentiation. An infection causes NK cells, macrophages, and T cells to produce IL18, which are recognized by IL18R1 (63) and presumably the receptor associated protein IL18RAP, unique to cardiac adipose. The recognition of IL18 by its receptor induces the production of IFNG (63), enhancing the Th1 cell phenotype (59). IFNG also, increases IL18R production (64). Further propagation of the Th1 cell phenotype would then maintain IL12 receptors, like IL12RB2, which is unique to abdominal

adipose (59, 64). IFNG inhibits IL4 (64), preventing the inhibition of IL12RB2 by IL4, inhibiting Th2 phenotype expression (65). Fibrinogen like 2 (FGL2), unique to abdominal adipose, elicits Th2 expression (66) along with serine peptidase inhibitor, Kazal type 7 (SPINK7) (67), unique to abdominal adipose. Overall, the abdominal adipose appears to have T-cells, both Th1 and Th2 whereas the cardiac adipose seems to lack in T-cell regulation, besides the presence of IL4.

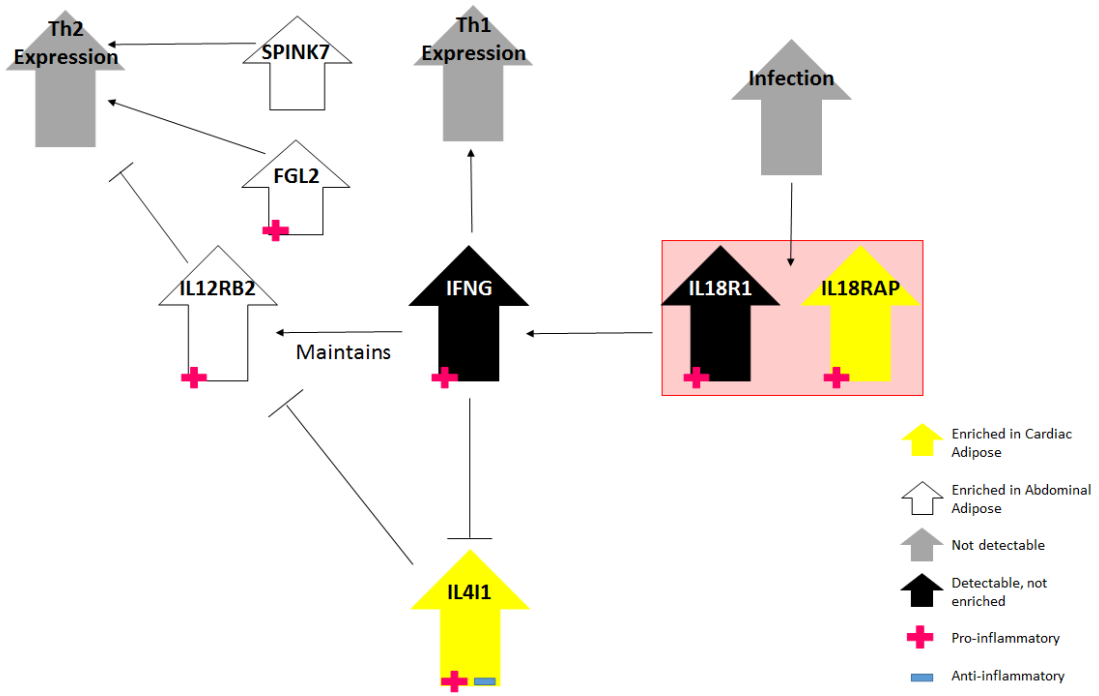

Figure 15: This figure displays the effects of IFNG and how Th1 and Th2 differentiation are affected. The genes enriched in cardiac adipose, abdominal adipose, and/or both are indicated in yellow, white, and red respectively. The plus signs indicate pro-inflammatory cytokines and the minus signs indicated anti-inflammatory cytokines. While this data is a good indication at what is going on in adipose tissue, another important thing to note is we are looking at the mRNA expression and this cannot be directly viewed as what is going on at the protein level.

Figure 16 demonstrates the inhibitory effects of ubiquitin specific peptidase 18 (USP18), an enzyme that de-ubiquitinates substrates and an overlapping gene, reflecting a dampening or control over the immune response being produced in the adipose. USP18 inhibits the mitogen-activated protein kinase kinase kinase 7 (MAP3K7)/TGF-beta activated kinase 1 (MAP3K7) binding protein 1 (TAB1) complex through de-ubiquitination, which is responsible for activating nuclear factor kappa-B (NFKB), a transcription regulator, and nuclear factor of activated T-cells 1 (NFATC1), a nuclear marker for T cell differentiation (68). USP18 prevents T cell differentiation. USP18 is also, in a negative feedback loop with interferon alpha (IFNA) and interferon beta (IFNB), a cardiac adipose unique gene, which are both pro-inflammatory cytokines (55) and type one interferons (69); USP18 inhibits IFNA and IFNB (70) and IFNB upregulates USP18, as an inhibitor (71). Some of the overall effects of IFNA and IFNB are increased infection resistance (72), activation of the JAK/STAT pathway (73), which is involved in multiple signaling cascades some of which include cytokine secretion and apoptosis (74), and increased inflammatory cytokines (75). In, addition type one interferons, such as IFNA and IFNB, increase the expression of MX dynamin like GTPase 1 (MX1), a GTPase unique to cardiac adipose, (76) and LOC416147, the chicken equivalent to ISG15 ubiquitin-like modifier (ISG15), a protein similar to ubiquitin (77). Both of these genes are involved in eliciting an antiviral response. Overall, it appears as though the role that USP18 plays is to turn off or lessen the adipose elicited immune response, which appears to be more prominent in the cardiac adipose. It would be hypothesized that this is the case because out of all of the body the heart is probably one of the worst places to get an infection.

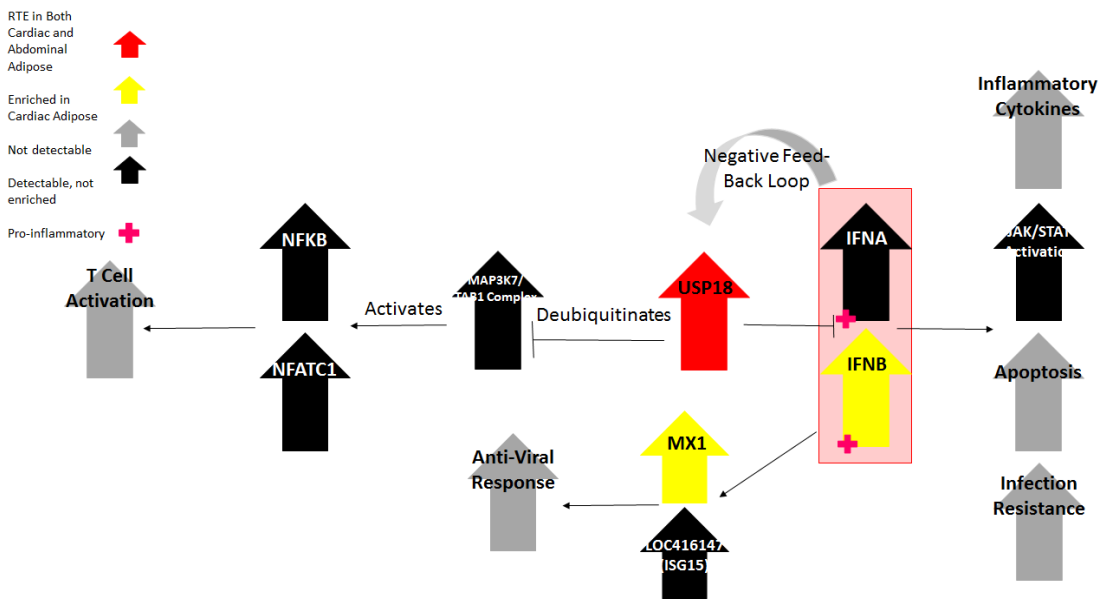

Figure 16: This figure displays the inhibitory effects of USP18, ultimately dampening the immune response. The immune responses inhibited appear to be more prominent in the cardiac adipose in comparison to the abdominal adipose. The genes enriched in cardiac adipose, abdominal adipose, and/or both are indicated in yellow, white, and red respectively. The plus signs indicate pro-inflammatory cytokines and the minus signs indicated anti-inflammatory cytokines. While this data is a good indication at what is going on in adipose tissue, another important thing to note is we are looking at the mRNA expression and this cannot be directly viewed as what is going on at the protein level.

Additionally, pentraxin 3 (PTX3), whose expression is induced by inflammation and then goes on to regulate inflammation, is unique to cardiac adipose is also probably involved in an innate immune response. PTX3 plays a role in initiating pathogen rejection (78), decreasing neutrophil recruitment with inflammation (79), and increasing phagocyte pathogen recognition (80). PTX3 is also shown to inhibit leukocyte invasion to the heart (81). Regulation of inflammatory responses and clearing of apoptotic cells are more effects of PTX3 expression (82).

Low pH increases levels of stabilin 1 (STAB1), a gene involved in endocytosis and unique to cardiac adipose tissue, leading to the increased clearing of apoptotic cells (83). IL4, which is unique to the cardiac adipose, on the other hand protects against apoptosis, through promoting cell survival, proliferation, and lymphogenesis (84). The overall, effect in the cardiac adipose appears to be a suppression of apoptosis accompanied by an increase in the clearing of apoptotic cells.

Adiponectin, C1Q and collagen domain containing (ADIPOQ), a gene involved in metabolic and hormone regulation that is unique to abdominal adipose, is linked to preventing inflammation. ADIPOQ along with IL10, a cytokine with both pro and anti- inflammatory responses (55), decrease IL6 levels and increase nuclear factor kappa-B (NFKB) binding to DNA, decreasing the inflammatory response (85). ADIPOQ also reduces angiotensin II specific inflammation (86); it should be noted that both angiotensin II receptor type 1 (AGTR1) and angiotensin II receptor type 2 (AGTR2) are overlapping genes. ADIPOQ reduces eosinophil adhesion (87), dampening the immune response further. This would indicate a balance of inflammation, subduing many of the other pro-inflammatory pathways indicated earlier in the abdominal adipose.

Poly (ADP-ribose) polymerase family member 14 (PARP14) is an anti-apoptotic gene and unique to the abdominal adipose. Cysteine rich angiogenic inducer 61 (CYR61), a gene involved in promoting endothelial adhesion unique to abdominal adipose, over-expression in mice decreases cell death (88). FGL2, which is unique to abdominal adipose, expression however induces apoptosis (89). CYR61 also regulates inflammation and fibrogenesis (90), an essential part of wound healing. Thus, in the abdominal adipose it appears that apoptosis is being suppressed. Figure 17

summarizes the effects on apoptosis by the unique adipose, abdominal and cardiac, genes with both types of adipose suppressing apoptosis but, through different mechanisms.

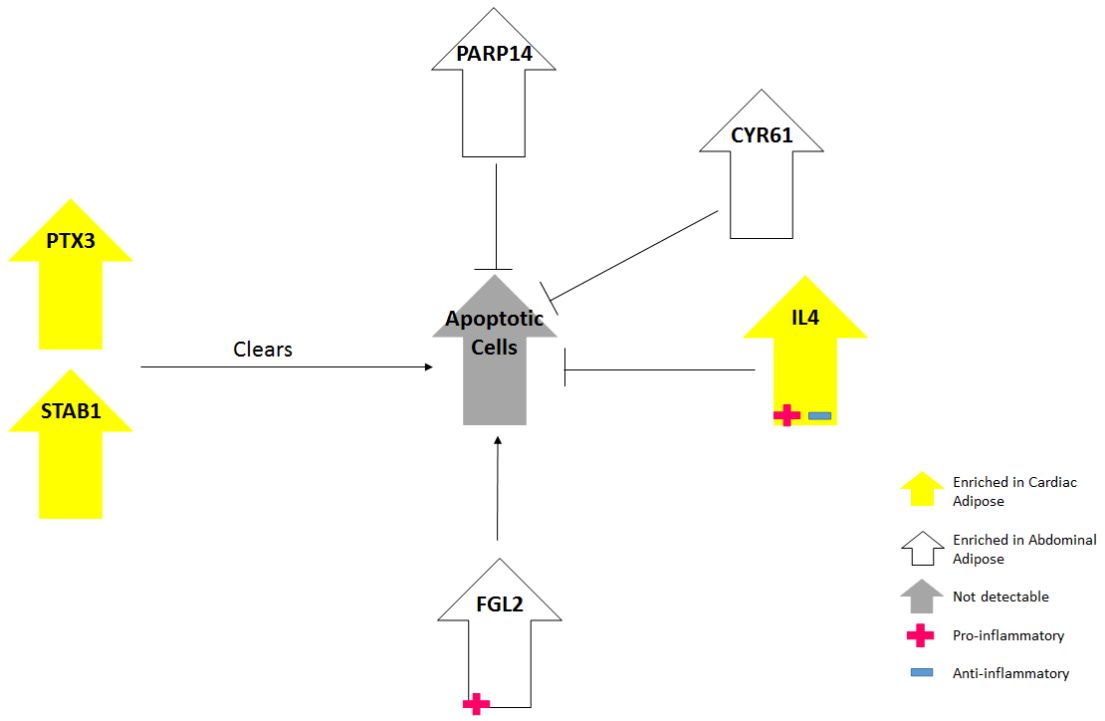

Figure 17: This figure summarizes how the unique abdominal and cardiac adipose genes affect apoptosis. Both types of adipose appear to suppress apoptosis but, utilize different pathways to do so. The genes enriched in cardiac adipose, abdominal adipose, and/or both are indicated in yellow, white, and red respectively. The plus signs indicate pro-inflammatory cytokines and the minus signs indicated anti-inflammatory cytokines. While this data is a good indication at what is going on in adipose tissue, another important thing to note is we are looking at the mRNA expression and this cannot be directly viewed as what is going on at the protein level.

Figure 18 depicts endocytosis regulation and inhibition of cell proliferation by caveolae. While, there is an overlapping gene involved in this pathway it is more relevant and unique to the abdominal adipose. Polymerase I and transcript release factor (PTRF) is a gene whose product is responsible for the formation and stabilization of caveolae, lipid microdomains involved in endocytosis, (91) and is unique to abdominal adipose. Caveolae are composed of caveolin 1 (CAV1), an overlapping gene, and caveolin 2 (CAV2), unique to abdominal adipose. CAV1 stabilizes CAV2, which in turn regulates endocytosis (92). Caveolae are also involved in promoting ECM recycling (93) with CAV2 also inhibiting cell proliferation (92). Finally, CAV1 is also, involved in decreasing fluid endocytosis (94). Overall, there is a display of endocytosis regulation balanced between CAV1 and CAV2. The regulation of endocytosis could be very important especially in the abdominal adipose, being the primary lipid storage depot of the body (6). Receptor mediated endocytosis is how LPL transports LDLs; this together with the upregulation of endocytosis could explain the growth of the abdominal fat pad.

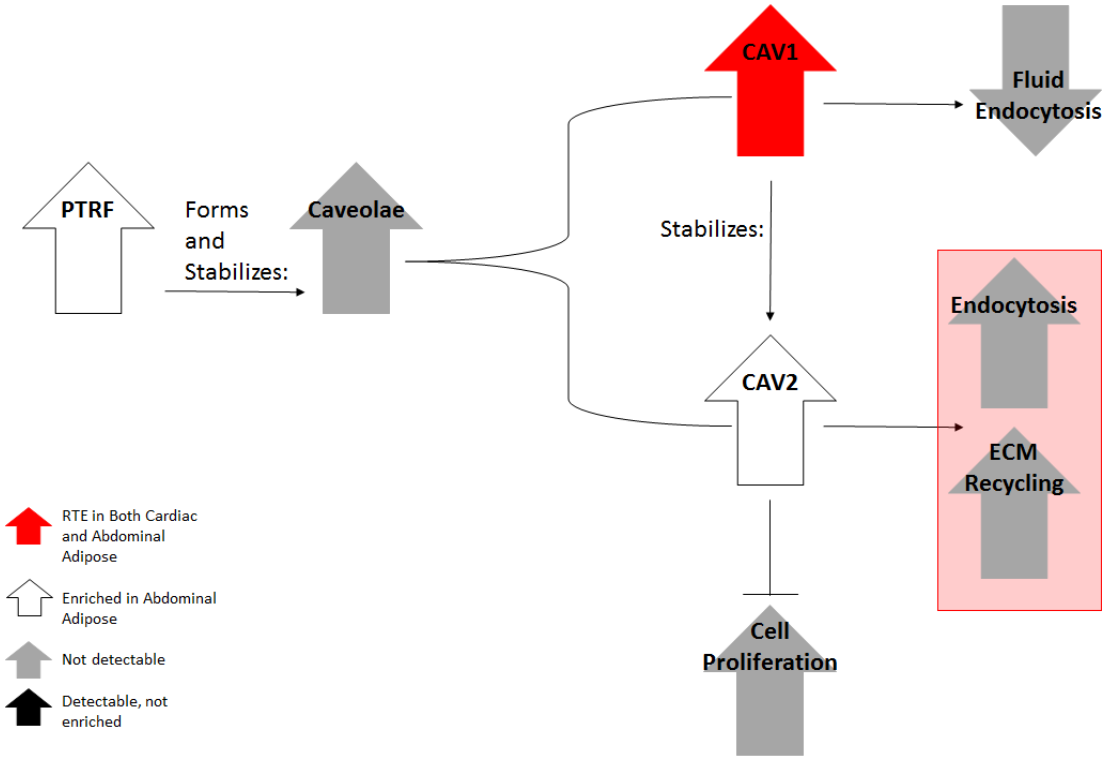

Figure 18: This figure displays the effects of caveolae and how endocytosis is regulated. This pathway is more enriched in the abdominal adipose in comparison to the cardiac adipose of the modern broiler chicken, as no cardiac genes take place in this pathway although CAV1 is an overlapping enriched gene. The genes enriched in cardiac adipose, abdominal adipose, and/or both are indicated in yellow, white, and red respectively. While this data is a good indication at what is going on in adipose tissue, another important thing to note is we are looking at the mRNA expression and this cannot be directly viewed as what is going on at the protein level.

Additionally, in response to inflammation prostaglandin E2 activates prostaglandin E receptor 3 (PTGER3), an overlapping gene and prostaglandin E receptor 4 (PTGER4), unique to abdominal adipose, which then recruit mast cells to the ECM (95). PTGER4 also regulates chemokine expression (96). Stabilin 1 (STAB1), a membrane receptor unique to cardiac adipose, is expressed in alternatively

activated macrophages and induces endocytosis clearing itself from the ECM when bound by secreted protein acidic and cysteine rich (SPARC), a ECM regulatory gene that induces deadhesion (97). Growth differentiation factor 7 (GDF7), a member of the TGFB family of ligands unique to cardiac adipose, was shown to aid in tendon healing through a switch from fibroblast production to the production of fibrocysts and decrease the number of adipocytes (98).

Overall, in the immune system pathway it appears as though there are unique ways in which the abdominal adipose and cardiac adipose handle inflammation with the abdominal adipose appearing slightly more pro-inflammatory. The cardiac adipose seems to be dampening the inflammatory response. The abdominal adipose appears to contain T-cells where the cardiac adipose does not. Apoptosis regulation mechanisms were suggested for each type of adipose. An increase in endocytosis is suggested in the abdominal adipose that could potentially be indicative to its function as the primary lipid storage depot.

Chapter 4

CONCLUSION

To conclude, abdominal and cardiac adipose function as an energy source in the same way within the broiler chicken. The extracellular matrix appears to be more static in the cardiac adipose. Cardiac adipose unique genes were identified that could possibly be related regulation of the aorta. The abdominal adipose appears to be slightly more pro-inflammatory whereas the cardiac adipose seems to be dampening inflammation. Finally, the abdominal adipose seems to contain T-cells and an enriched endocytosis pathway, emphasizing its role as the primary lipid storage depot. The transcriptome data for the broiler abdominal and cardiac adipose tissue offers a solid point of comparison for future studies including to comparison to legacy lines and stressed chickens. To make this study more complete, future work would include validation by quantitative real time polymerase chain reaction (qRT-PCR) validation of enriched genes, proteomics, to see if the proteins and not just the transcripts are present, and metabolomics, to gain a better understanding of the metabolic processes that are taking place particularly, at the lipid level. Seeing the difference in lipid content between the two types of adipose could also potentially highlight some of the differences in functioning. Overall, this work sets a solid foundation to base future studies on.

REFERENCES

1. Maurice Goodman H. Basic Medical Endocrinology [Internet]. Academic Press; 2010. Available from: https://market.android.com/details?id=book-gjpi2MYVKGAC

2. Lopaschuk GD, Ussher JR, Folmes CDL, Jaswal JS, Stanley WC. Myocardial fatty acid metabolism in health and disease. Physiol Rev [Internet] 2010;90(1):207–58. Available from: http://dx.doi.org/10.1152/physrev.00015.2009

3. Sacks HS, Fain JN. Human epicardial adipose tissue: A review. Am Heart J [Internet] 2007; 153(6):907–17. Available from: http://dx.doi.org/10.1016/j.ahj.2007.03.019

4. Marchington JM, Mattacks CA, Pond CM. Adipose tissue in the mammalian heart and pericardium: structure, foetal development and biochemical properties. Comp Biochem Physiol B [Internet] 1989; 94(2):225–32. Available from: https://www.ncbi.nlm.nih.gov/pubmed/2591189

5. Marchington JM, Pond CM. Site-specific properties of pericardial and epicardial adipose tissue: the effects of insulin and high-fat feeding on lipogenesis and the incorporation of fatty acids in vitro. Int J Obes [Internet] 1990; 14(12):1013–22. Available from: https://www.ncbi.nlm.nih.gov/pubmed/2086494

6. Muret K, Klopp C, Wucher V, et al. Long noncoding RNA repertoire in chicken liver and adipose tissue. Genet Sel Evol [Internet] 2017; 49(1):6. Available from: http://dx.doi.org/10.1186/s12711-016-0275-0

7. Huh JY, Park YJ, Ham M, Kim JB. Crosstalk between adipocytes and immune cells in adipose tissue inflammation and metabolic dysregulation in obesity. Mol Cells [Internet] 2014; 37(5):365–71. Available from: http://dx.doi.org/10.14348/molcells.2014.0074

8. Weisberg SP, McCann D, Desai M, Rosenbaum M, Leibel RL, Ferrante AW. Obesity is associated with macrophage accumulation in adipose tissue. J Clin Invest [Internet] 2003; 112(12):1796–808. Available from: http://dx.doi.org/10.1172/jci19246

9. Schurch NJ, Schofield P, Gierliński M, et al. Erratum: How many biological replicates are needed in an RNA-seq experiment and which differential expression tool should you use? RNA [Internet] 2016; 22(10):1641–1641. Available from: http://dx.doi.org/10.1261/rna.058339.116

10. Bailey MJ, Coon SL, Carter DA, et al. Night/day changes in pineal expression of >600 genes: central role of adrenergic/cAMP signaling. J Biol Chem [Internet] 2009; 284(12):7606–22. Available from: http://dx.doi.org/10.1074/jbc.M808394200

11. Carbon S, Ireland A, Mungall CJ, et al. AmiGO: online access to ontology and annotation data. Bioinformatics [Internet] 2009; 25(2):288–9. Available from: http://dx.doi.org/10.1093/bioinformatics/btn615

12. Zhu Y, Sun L, Garbarino A, Schmidt C, Fang J, Chen J. PathRings: a web-based tool for exploration of ortholog and expression data in biological pathways. BMC Bioinformatics [Internet] 2015; 16:165. Available from: http://dx.doi.org/10.1186/s12859-015-0585-1

13. Sun L, Zhu Y, Mahmood ASMA, et al. WebGIVI: a web-based gene enrichment analysis and visualization tool. BMC Bioinformatics [Internet] 2017;18(1):237. Available from: http://dx.doi.org/10.1186/s12859-017-1664-2

14. Fajas L, Fruchart JC, Auwerx J. Transcriptional control of adipogenesis. Curr Opin Cell Biol [Internet] 1998; 10(2):165–73. Available from: https://www.ncbi.nlm.nih.gov/pubmed/9561840

15. Garin-Shkolnik T, Rudich A, Hotamisligil GS, Rubinstein M. FABP4 attenuates PPARγ and adipogenesis and is inversely correlated with PPARγ in adipose tissues. Diabetes [Internet] 2014; 63(3):900–11. Available from: http://dx.doi.org/10.2337/db13-0436

16. Griffin MJ, Zhou Y, Kang S, Zhang X, Mikkelsen TS, Rosen ED. Early B-cell Factor-1 (EBF1) Is a Key Regulator of Metabolic and Inflammatory Signaling Pathways in Mature Adipocytes. J Biol Chem [Internet] 2013; 288(50):35925–39. Available from: http://dx.doi.org/10.1074/jbc.m113.491936

17. Jimenez MA, Akerblad P, Sigvardsson M, Rosen ED. Critical role for Ebf1 and Ebf2 in the adipogenic transcriptional cascade. Mol Cell Biol [Internet] 2007;27(2):743–57. Available from: http://dx.doi.org/10.1128/MCB.01557-06

18. Atsawasuwan P, Mochida Y, Katafuchi M, et al. Lysyl Oxidase Binds Transforming Growth Factor- and Regulates Its Signaling via Amine Oxidase Activity. J Biol Chem [Internet] 2008; 283(49):34229–40. Available from: http://dx.doi.org/10.1074/jbc.m803142200

19. Goto Y, Uchio-Yamada K, Anan S, Yamamoto Y, Ogura A, Manabe N. Transforming growth factor-beta1 mediated up-regulation of lysyl oxidase in the kidneys of hereditary nephrotic mouse with chronic renal fibrosis. Virchows Arch [Internet] 2005; 447(5):859–68. Available from: http://dx.doi.org/10.1007/s00428-005-0001-8

20. Horiguchi M, Inoue T, Ohbayashi T, et al. Fibulin-4 conducts proper elastogenesis via interaction with cross-linking enzyme lysyl oxidase. Proc Natl Acad Sci U S A [Internet] 2009; 106(45):19029–34. Available from: http://dx.doi.org/10.1073/pnas.0908268106

21. Lemaire R, Bayle J, Mecham RP, Lafyatis R. Microfibril-associated MAGP-2 stimulates elastic fiber assembly. J Biol Chem [Internet] 2007; 282(1):800–8. Available from: http://dx.doi.org/10.1074/jbc.M609692200

22. Soskel NT, Watanabe S, Hammond E, Sandberg LB, Renzetti AD Jr, Crapo JD. A copper-deficient, zinc-supplemented diet produces emphysema in pigs. Am Rev Respir Dis [Internet] 1982; 126(2):316–25. Available from: http://dx.doi.org/10.1164/arrd.1982.126.2.316

23. Penner AS, Rock MJ, Kielty CM, Shipley JM. Microfibril-associated glycoprotein-2 interacts with fibrillin-1 and fibrillin-2 suggesting a role for MAGP-2 in elastic fiber assembly. J Biol Chem [Internet] 2002; 277(38):35044–9. Available from: http://dx.doi.org/10.1074/jbc.M206363200

24. Wang W-M, Ge G, Lim NH, Nagase H, Greenspan DS. TIMP-3 inhibits the procollagen N-proteinase ADAMTS-2. Biochem J [Internet] 2006;398(3):515–9. Available from: http://dx.doi.org/10.1042/BJ20060630

25. Wang W-M, Lee S, Steiglitz BM, et al. Transforming Growth Factor- Induces Secretion of Activated ADAMTS-2: A PROCOLLAGEN III N-PROTEINASE. J Biol Chem [Internet] 2003; 278(21):19549–57. Available from: http://dx.doi.org/10.1074/jbc.m300767200

26. Voloshenyuk TG, Hart AD, Khoutorova E, Gardner JD. TNF-α increases cardiac fibroblast lysyl oxidase expression through TGF-β and PI3Kinase signaling pathways. Biochem Biophys Res Commun [Internet] 2011; 413(2):370–5. Available from: http://dx.doi.org/10.1016/j.bbrc.2011.08.109

27. Lemaire R, Korn JH, Shipley JM, Lafyatis R. Increased expression of type I collagen induced by microfibril-associated glycoprotein 2: novel mechanistic insights into the molecular basis of dermal fibrosis in scleroderma. Arthritis Rheum [Internet] 2005; 52(6):1812–23. Available from: http://dx.doi.org/10.1002/art.21059

28. Furuzawa-Carballeda J, Muñoz-Chablé OA, Barrios-Payán J, Hernández-Pando R. Effect of polymerized-type I collagen in knee osteoarthritis. I. In vitro study. Eur J Clin Invest [Internet] 2009; 39(7):591–7. Available from: http://dx.doi.org/10.1111/j.1365-2362.2009.02154.x

29. Tian H, Stogiannidis I. Up-regulation of Cartilage Oligomeric Matrix Protein Gene Expression by Insulin-like Growth Factor-I Revealed by Real Time Reverse Transcription-Polymerase Chain Reaction. Acta Biochim Biophys Sin [Internet] 2006; 38(10):677–82. Available from: http://dx.doi.org/10.1111/j.1745-7270.2006.00218.x

30. Posey KL, Coustry F, Veerisetty AC, Liu P, Alcorn JL, Hecht JT. Chop (Ddit3) Is Essential for D469del-COMP Retention and Cell Death in Chondrocytes in an Inducible Transgenic Mouse Model of Pseudoachondroplasia. Am J Pathol [Internet] 2012; 180(2):727–37. Available from: http://dx.doi.org/10.1016/j.ajpath.2011.10.035

31. Nakahama M, Murakami T, Kusachi S, et al. Expression of perlecan proteoglycan in the infarct zone of mouse myocardial infarction. J Mol Cell Cardiol [Internet] 2000; 32(6):1087–100. Available from: http://dx.doi.org/10.1006/jmcc.2000.1146

32. Mariencheck MC, Davis EC, Zhang H, et al. Fibrillin-1 and fibrillin-2 show temporal and tissue-specific regulation of expression in developing elastic tissues. Connect Tissue Res [Internet] 1995;31(2):87–97. Available from: https://www.ncbi.nlm.nih.gov/pubmed/15612324

33. Coral K, Angayarkanni N, Madhavan J, et al. Lysyl oxidase activity in the ocular tissues and the role of LOX in proliferative diabetic retinopathy and rhegmatogenous retinal detachment. Invest Ophthalmol Vis Sci [Internet] 2008; 49(11):4746–52. Available from: http://dx.doi.org/10.1167/iovs.07-1550

34. Lord MS, Jung M, Cheng B, Whitelock JM. Transcriptional complexity of the HSPG2 gene in the human mast cell line, HMC-1. Matrix Biol [Internet] 2014; 35:123–31. Available from: http://dx.doi.org/10.1016/j.matbio.2013.12.005

35. Bax DV, Bernard SE, Lomas A, et al. Cell Adhesion to Fibrillin-1 Molecules and Microfibrils Is Mediated by 5 1 and v 3 Integrins. J Biol Chem [Internet] 2003; 278(36):34605–16. Available from: http://dx.doi.org/10.1074/jbc.m303159200

36. Sugitani H, Wachi H, Tajima S, Seyama Y. Nitric oxide stimulates elastin expression in chick aortic smooth muscle cells. Biol Pharm Bull [Internet] 2001; 24(5):461–4. Available from: https://www.ncbi.nlm.nih.gov/pubmed/11379760

37. Robinson PN, Booms P. Human Genome and Diseases:¶The molecular pathogenesis of the Marfan syndrome. Cell Mol Life Sci [Internet] 2001; 58(11):1698–707. Available from: http://dx.doi.org/10.1007/pl00000807

38. Carta L, Smaldone S, Zilberberg L, et al. p38 MAPK is an early determinant of promiscuous Smad2/3 signaling in the aortas of fibrillin-1 (Fbn1)-null mice. J Biol Chem [Internet] 2009; 284(9):5630–6. Available from: http://dx.doi.org/10.1074/jbc.M806962200

39. Albig AR, Roy TG, Becenti DJ, Schiemann WP. Transcriptome analysis of endothelial cell gene expression induced by growth on matrigel matrices: identification and characterization of MAGP-2 and lumican as novel regulators of angiogenesis. Angiogenesis [Internet] 2007; 10(3):197–216. Available from: http://dx.doi.org/10.1007/s10456-007-9075-z

40. Yoshida K, Murata M, Yamaguchi T, Matsuzaki K. TGF-β/Smad signaling during hepatic fibro-carcinogenesis (review). Int J Oncol [Internet] 2014; 45(4):1363–71. Available from: http://dx.doi.org/10.3892/ijo.2014.2552

41. Velasco J, Li J, DiPietro L, Stepp MA, Sandy JD, Plaas A. Adamts5 Deletion Blocks Murine Dermal Repair through CD44-mediated Aggrecan Accumulation and Modulation of Transforming Growth Factor 1 (TGF 1) Signaling. J Biol Chem [Internet] 2011; 286(29):26016–27. Available from: http://dx.doi.org/10.1074/jbc.m110.208694

42. Kizawa H, Kou I, Iida A, et al. An aspartic acid repeat polymorphism in asporin inhibits chondrogenesis and increases susceptibility to osteoarthritis. Nat Genet [Internet] 2005; 37(2):138–44. Available from: http://dx.doi.org/10.1038/ng1496

43. Kou I, Nakajima M, Ikegawa S. Binding characteristics of the osteoarthritis-associated protein asporin. J Bone Miner Metab [Internet] 2010; 28(4):395–402. Available from: http://dx.doi.org/10.1007/s00774-009-0145-8

44. Kou I, Nakajima M, Ikegawa S. Expression and regulation of the osteoarthritis-associated protein asporin. J Biol Chem [Internet] 2007; 282(44):32193–9. Available from: http://dx.doi.org/10.1074/jbc.M706262200

45. González GE, Rhaleb N-E, Nakagawa P, et al. N -acetyl-seryl-aspartyl-lysyl-proline reduces cardiac collagen cross-linking and inflammation in angiotensin II-induced hypertensive rats. Clin Sci [Internet] 2014; 126(1):85–94. Available from: http://dx.doi.org/10.1042/cs20120619

46. Kim DJ, Lee DC, Yang S-J, et al. Lysyl oxidase like 4, a novel target gene of TGF-β1 signaling, can negatively regulate TGF-β1-induced cell motility in PLC/PRF/5 hepatoma cells. Biochem Biophys Res Commun [Internet] 2008; 373(4):521–7. Available from: http://dx.doi.org/10.1016/j.bbrc.2008.06.071

47. Ogawa N, Imai Y, Nishimura H, et al. Circulating transforming growth factor β-1 level in Japanese patients with Marfan syndrome. Int Heart J [Internet] 2013;54(1):23–6. Available from: https://www.ncbi.nlm.nih.gov/pubmed/23428920

48. Mariko B, Pezet M, Escoubet B, et al. Fibrillin-1 genetic deficiency leads to pathological ageing of arteries in mice. J Pathol [Internet] 2011;224(1):33–44. Available from: http://dx.doi.org/10.1002/path.2840

49. Orriols M, Guadall A, Galán M, et al. Lysyl oxidase (LOX) in vascular remodelling. Insight from a new animal model. Thromb Haemost [Internet] 2014; 112(4):812–24. Available from: http://dx.doi.org/10.1160/TH14-01-0024

50. Walker HA. Perlecan Up-Regulation of FRNK Suppresses Smooth Muscle Cell Proliferation via Inhibition of FAK Signaling. Mol Biol Cell [Internet] 2003; 14(5):1941–52. Available from: http://dx.doi.org/10.1091/mbc.e02-08-0508

51. Crisan M, Yap S, Casteilla L, et al. A perivascular origin for mesenchymal stem cells in multiple human organs. Cell Stem Cell [Internet] 2008; 3(3):301–13. Available from: http://dx.doi.org/10.1016/j.stem.2008.07.003

52. Baumgartl H-J, Standl E. The atherosclerotic process and its exacerbation by diabetes. Exp Clin Endocrinol Diabetes [Internet] 2001; 109(Suppl 2):S487–92. Available from: http://dx.doi.org/10.1055/s-2001-18604

53. DeCarlo AA, Whitelock JM. The role of heparan sulfate and perlecan in bone-regenerative procedures. J Dent Res [Internet] 2006; 85(2):122–32. Available from: http://dx.doi.org/10.1177/154405910608500203

54. Wang Z-Q, Xing W-M, Fan H-H, et al. The Novel Lipopolysaccharide-Binding Protein CRISPLD2 Is a Critical Serum Protein to Regulate Endotoxin Function. The Journal of Immunology [Internet] 2009; 183(10):6646–56. Available from: http://dx.doi.org/10.4049/jimmunol.0802348

55. Seruga B, Zhang H, Bernstein LJ, Tannock IF. Cytokines and their relationship to the symptoms and outcome of cancer. Nat Rev Cancer [Internet] 2008; 8(11):887–99. Available from: http://dx.doi.org/10.1038/nrc2507

56. Li K, Dan Z, Hu X, et al. CD14 overexpression upregulates TNF-α-mediated inflammatory responses and suppresses the malignancy of gastric carcinoma cells. Mol Cell Biochem [Internet] 2013; 376(1-2):137–43. Available from: http://dx.doi.org/10.1007/s11010-013-1559-0

57. de Paus RA, Geilenkirchen MA, van Riet S, van Dissel JT, van de Vosse E. Differential expression and function of human IL-12Rβ2 polymorphic variants. Mol Immunol [Internet] 2013; 56(4):380–9. Available from: http://dx.doi.org/10.1016/j.molimm.2013.07.002

58. Jäger A, Kuchroo VK. Effector and Regulatory T-cell Subsets in Autoimmunity and Tissue Inflammation. Scand J Immunol [Internet] 2010; 72(3):173–84. Available from: http://dx.doi.org/10.1111/j.1365-3083.2010.02432.x

59. Paul WE. Fundamental Immunology [Internet]. Lippincott Williams & Wilkins; 1999. Available from: https://books.google.com/books/about/Fundamental_Immunology.html?hl=&id=WLY0MQAACAAJ

60. Zhang J, Shan L, Koussih L, et al. Pentraxin 3 (PTX3) expression in allergic asthmatic airways: role in airway smooth muscle migration and chemokine production. PLoS One [Internet] 2012; 7(4):e34965. Available from: http://dx.doi.org/10.1371/journal.pone.0034965

61. Kedda M-A. The CD14 C-159T polymorphism is not associated with asthma or asthma severity in an Australian adult population. Thorax [Internet] 2005;60(3):211–4. Available from: http://dx.doi.org/10.1136/thx.2004.028449

62. Caspar-Bauguil S, Cousin B, Bour S, Castiella L, Penicaud L, Carpéné C. Adipose tissue lymphocytes: types and roles. J Physiol Biochem [Internet] 2009; 65(4):423–36. Available from: http://dx.doi.org/10.1007/bf03185938

63. Neumann D, Martin MU. Interleukin-12 upregulates the IL-18Rbeta chain in BALB/c thymocytes. J Interferon Cytokine Res [Internet] 2001; 21(8):635–42. Available from: http://dx.doi.org/10.1089/10799900152547902

64. Smeltz RB, Chen J, Ehrhardt R, Shevach EM. Role of IFN-gamma in Th1 differentiation: IFN-gamma regulates IL-18R alpha expression by preventing the negative effects of IL-4 and by inducing/maintaining IL-12 receptor beta 2 expression. J Immunol [Internet] 2002; 168(12):6165–72. Available from: https://www.ncbi.nlm.nih.gov/pubmed/12055229

65. Szabo SJ, Dighe AS, Gubler U, Murphy KM. Regulation of the Interleukin (IL)-12R β2 Subunit Expression in Developing T Helper 1 (Th1) and Th2 Cells. J Exp Med [Internet] 1997; 185(5):817–24. Available from: http://dx.doi.org/10.1084/jem.185.5.817

66. Joller N, Lozano E, Burkett PR, et al. Treg cells expressing the coinhibitory molecule TIGIT selectively inhibit proinflammatory Th1 and Th17 cell responses. Immunity [Internet] 2014; 40(4):569–81. Available from: http://dx.doi.org/10.1016/j.immuni.2014.02.012

67. Rupa P, Mine Y. Engineered recombinant ovomucoid third domain can desensitize Balb/c mice of egg allergy. Allergy [Internet] 2006; 61(7):836–42. Available from: http://dx.doi.org/10.1111/j.1398-9995.2006.01143.x

68. Liu X, Li H, Zhong B, et al. USP18 inhibits NF-κB and NFAT activation during Th17 differentiation by deubiquitinating the TAK1-TAB1 complex. J Exp Med [Internet] 2013; 210(8):1575–90. Available from: http://dx.doi.org/10.1084/jem.20122327

69. Samarajiwa SA, Forster S, Auchettl K, Hertzog PJ. INTERFEROME: the database of interferon regulated genes. Nucleic Acids Res [Internet] 2009; 37(Database issue):D852–7. Available from: http://dx.doi.org/10.1093/nar/gkn732

70. Yim HY, Yang Y, Lim J-S, Lee MS, Zhang D-E, Kim KI. The mitochondrial pathway and reactive oxygen species are critical contributors to interferon-α/β-mediated apoptosis in Ubp43-deficient hematopoietic cells. Biochem Biophys Res Commun [Internet] 2012; 423(2):436–40. Available from: http://dx.doi.org/10.1016/j.bbrc.2012.05.154

71. Colonne PM, Sahni A, Sahni SK. Suppressor of cytokine signalling protein SOCS1 and UBP43 regulate the expression of type I interferon-stimulated genes in human microvascular endothelial cells infected with Rickettsia conorii. J Med Microbiol [Internet] 2013; 62(Pt 7):968–79. Available from: http://dx.doi.org/10.1099/jmm.0.054502-0

72. Yan M, Luo J-K, Ritchie KJ, et al. Ubp43 regulates BCR-ABL leukemogenesis via the type 1 interferon receptor signaling. Blood [Internet] 2007; 110(1):305–12. Available from: http://dx.doi.org/10.1182/blood-2006-07-033209

73. Cong X-L, Lo M-C, Reuter BA, Yan M, Fan J-B, Zhang D-E. Usp18 promotes conventional CD11b+ dendritic cell development. J Immunol [Internet] 2012; 188(10):4776–81. Available from: http://dx.doi.org/10.4049/jimmunol.1101609

74. Rawlings JS, Rosler KM, Harrison DA. The JAK/STAT signaling pathway. J Cell Sci [Internet] 2004; 117(Pt 8):1281–3. Available from: http://dx.doi.org/10.1242/jcs.00963

75. Dauphinee SM, Richer E, Eva MM, et al. Contribution of increased ISG15, ISGylation and deregulated type I IFN signaling in Usp18 mutant mice during the course of bacterial infections. Genes Immun [Internet] 2014; 15(5):282–92. Available from: http://dx.doi.org/10.1038/gene.2014.17

76. Moritoh K, Yamauchi H, Asano A, et al. Generation of congenic mouse strains by introducing the virus-resistant genes, Mx1 and Oas1b, of feral mouse-derived inbred strain MSM/Ms into the common strain C57BL/6J. Jpn J Vet Res [Internet] 2009; 57(2):89–99. Available from: https://www.ncbi.nlm.nih.gov/pubmed/19827744

77. Li S, Duan X, Li Y, Liu B, McGilvray I, Chen L. MicroRNA-130a inhibits HCV replication by restoring the innate immune response. J Viral Hepat [Internet] 2014; 21(2):121–8. Available from: http://dx.doi.org/10.1111/jvh.12131

78. Garlanda C, Bottazzi B, Moalli F, et al. Pentraxins and atherosclerosis: the role of PTX3. Curr Pharm Des [Internet] 2011; 17(1):38–46. Available from: https://www.ncbi.nlm.nih.gov/pubmed/21226667

79. Deban L, Castro Russo R, Sironi M, et al. Regulation of leukocyte recruitment by the long pentraxin PTX3. Nat Immunol [Internet] 2010;11(4):328–34. Available from: http://dx.doi.org/10.1038/ni.1854

80. Bottazzi B. The long pentraxin PTX3 as a link among innate immunity, inflammation, and female fertility. J Leukoc Biol [Internet] 2006; 79(5):909–12. Available from: http://dx.doi.org/10.1189/jlb.1005557

81. Voigt A, Possehl A, Klingel K, Rahnefeld A. P625An insight into the function of immunoproteasomes in immunmodulation: induction of the pattern recognition factor Pentraxin 3 in acute cardiac inflammation. Cardiovasc Res [Internet] 2014; 103(suppl 1):S113.3–S113. Available from: http://dx.doi.org/10.1093/cvr/cvu098.53

82. Okutani D. [The role of long pentraxin 3, a new inflammatory mediator in inflammatory responses]. Nihon Rinsho Meneki Gakkai Kaishi [Internet] 2006; 29(3):107–13. Available from: https://www.ncbi.nlm.nih.gov/pubmed/16819259

83. Park S-Y, Bae D-J, Kim M-J, Piao ML, Kim I-S. Extracellular Low pH Modulates Phosphatidylserine-dependent Phagocytosis in Macrophages by Increasing Stabilin-1 Expression. J Biol Chem [Internet] 2012; 287(14):11261–71. Available from: http://dx.doi.org/10.1074/jbc.m111.310953

84. Cho SH, Goenka S, Henttinen T, et al. PARP-14, a member of the B aggressive lymphoma family, transduces survival signals in primary B cells. Blood [Internet] 2009; 113(11):2416–25. Available from: http://dx.doi.org/10.1182/blood-2008-03-144121

85. Lira FS, Rosa JC, Pimentel GD, et al. Both adiponectin and interleukin-10 inhibit LPS-induced activation of the NF-κB pathway in 3T3-L1 adipocytes. Cytokine [Internet] 2012; 57(1):98–106. Available from: http://dx.doi.org/10.1016/j.cyto.2011.10.001

86. Qi G-M, Jia L-X, Li Y-L, Li H-H, Du J. Adiponectin suppresses angiotensin II-induced inflammation and cardiac fibrosis through activation of macrophage autophagy. Endocrinology [Internet] 2014; 155(6):2254–65. Available from: http://dx.doi.org/10.1210/en.2013-2011

87. Yamamoto R, Ueki S, Moritoki Y, et al. Adiponectin attenuates human eosinophil adhesion and chemotaxis: implications in allergic inflammation. J Asthma [Internet] 2013; 50(8):828–35. Available from: http://dx.doi.org/10.3109/02770903.2013.816725

88. Fromigue O, Hamidouche Z, Vaudin P, et al. CYR61 downregulation reduces osteosarcoma cell invasion, migration, and metastasis. J Bone Miner Res [Internet] 2011; 26(7):1533–42. Available from: http://dx.doi.org/10.1002/jbmr.343

89. Liu M, Mendicino M, Ning Q, et al. Cytokine-induced hepatic apoptosis is dependent on FGL2/fibroleukin: the role of Sp1/Sp3 and STAT1/PU.1 composite cis elements. J Immunol [Internet] 2006; 176(11):7028–38. Available from: https://www.ncbi.nlm.nih.gov/pubmed/16709865

90. Lau LF. CCN1/CYR61: the very model of a modern matricellular protein. Cell Mol Life Sci [Internet] 2011; 68(19):3149–63. Available from: http://dx.doi.org/10.1007/s00018-011-0778-3

91. Briand N, Dugail I, Le Lay S. Cavin proteins: New players in the caveolae field. Biochimie [Internet] 2011; 93(1):71–7. Available from: http://dx.doi.org/10.1016/j.biochi.2010.03.022

92. Razani B, Engelman JA, Wang XB, et al. Caveolin-1 null mice are viable but show evidence of hyperproliferative and vascular abnormalities. J Biol Chem [Internet] 2001; 276(41):38121–38. Available from: http://dx.doi.org/10.1074/jbc.M105408200

93. Aga M, Bradley JM, Wanchu R, Yang Y-F, Acott TS, Keller KE. Differential effects of caveolin-1 and -2 knockdown on aqueous outflow and altered extracellular matrix turnover in caveolin-silenced trabecular meshwork cells. Invest Ophthalmol Vis Sci [Internet] 2014; 55(9):5497–509. Available from: http://dx.doi.org/10.1167/iovs.14-14519

94. Cheng Z-J, Singh RD, Holicky EL, Wheatley CL, Marks DL, Pagano RE. Co-regulation of caveolar and Cdc42-dependent fluid phase endocytosis by phosphocaveolin-1. J Biol Chem [Internet] 2010; 285(20):15119–25. Available from: http://dx.doi.org/10.1074/jbc.M109.069427

95. Hatae N, Kita A, Tanaka S, Sugimoto Y, Ichikawa A. Induction of adherent activity in mastocytoma P-815 cells by the cooperation of two prostaglandin E2 receptor subtypes, EP3 and EP4. J Biol Chem [Internet] 2003; 278(20):17977–81. Available from: http://dx.doi.org/10.1074/jbc.M301312200

96. Zahner G, Schaper M, Panzer U, et al. Prostaglandin EP2 and EP4 receptors modulate expression of the chemokine CCL2 (MCP-1) in response to LPS-induced renal glomerular inflammation. Biochem J [Internet] 2009; 422(3):563–70. Available from: http://dx.doi.org/10.1042/BJ20090420

97. Workman G, Sage EH. Identification of a sequence in the matricellular protein SPARC that interacts with the scavenger receptor stabilin-1. J Cell Biochem [Internet] 2011; 112(4):1003–8. Available from: http://dx.doi.org/10.1002/jcb.23015

98. Majewski M, Betz O, Ochsner PE, Liu F, Porter RM, Evans CH. Ex vivo adenoviral transfer of bone morphogenetic protein 12 (BMP-12) cDNA improves Achilles tendon healing in a rat model. Gene Ther [Internet] 2008; 15(16):1139–46. Available from: http://dx.doi.org/10.1038/gt.2008.48